Re-evaluating pretomanid analogues for Chagas disease

Thompson, Andrew M.; O'Connor, Patrick D.; Marshall, Andrew J.; Francisco, Amanda F.; Kelly, John M.; Riley, Jennifer

Published in:
European Journal of Medicinal Chemistry

DOI:
10.1016/j.ejmech.2020.112849

Publication date:
2020

Re-evaluating pretomanid analogues for Chagas disease: hit-to-lead studies reveal both *in vitro* and *in vivo* trypanocidal efficacy

Andrew M. Thompson[a,*], Patrick D. O'Connor[a,1], Andrew J. Marshall[a,2], Amanda F. Francisco[b], John M. Kelly[b], Jennifer Riley[c], Kevin D. Read[c], Catherine J. Perez[d], Scott Cornwall[d,3], R. C. Andrew Thompson[d], Martine Keenan[e], Karen L. White[f], Susan A. Charman[f], Bilal Zulfiqar[g], Melissa L. Sykes[g], Vicky M. Avery[g], Eric Chatelain[h], William A. Denny[a]

[a]*Auckland Cancer Society Research Centre, School of Medical Sciences, The University of Auckland, Private Bag 92019, Auckland 1142, New Zealand;* [b]*Department of Infection Biology, London School of Hygiene & Tropical Medicine, Keppel Street, London WC1E 7HT, United Kingdom;* [c]*Drug Discovery Unit, School of Life Sciences, University of Dundee, Dow Street, Dundee DD1 5EH, United Kingdom;* [d]*Department of Parasitology & Veterinary Sciences, Murdoch University, South Street, Murdoch, Western Australia 6150, Australia;* [e]*Epichem Pty Ltd, Suite 5, 3 Brodie-Hall Drive, Technology Park, Bentley, Western Australia 6102, Australia;* [f]*Centre for Drug Candidate Optimisation, Monash University, 381 Royal Parade, Parkville, Victoria 3052, Australia;* [g]*Discovery Biology, Griffith Institute for Drug Discovery, Griffith University, Don Young Road, Nathan, Queensland 4111, Australia;* [h]*Drugs for Neglected Diseases initiative, 15 Chemin Louis Dunant, 1202 Geneva, Switzerland.*

Present addresses:

[1]Helmholtz Zentrum München, Ingolstädter Landstr. 1, 85764 Neuherberg, Germany
[2]Ferrier Research Institute, Victoria University of Wellington, 69 Gracefield Road, Lower Hutt 5010, New Zealand
[3]PathWest Laboratory Medicine, Locked Bag 2009, Nedlands, WA 6009, Australia

*Corresponding author: Dr Andrew M. Thompson, Auckland Cancer Society Research Centre, School of Medical Sciences, The University of Auckland. Ph: (+649) 923 6145. Email: am.thompson@auckland.ac.nz

Abstract

Phenotypic screening of a 900 compound library of antitubercular nitroimidazole derivatives related to pretomanid against the protozoan parasite *Trypanosoma cruzi* (the causative agent for Chagas disease) identified several structurally diverse hits with an unknown mode of action. Following initial profiling, a first proof-of-concept *in vivo* study was undertaken, in which once daily oral dosing of a 7-substituted 2-nitroimidazooxazine analogue suppressed blood parasitemia to low or undetectable levels, although sterile cure was not achieved. Limited hit expansion studies alongside counter-screening of new compounds targeted at visceral leishmaniasis laid the foundation for a more in-depth assessment of the best leads, focusing on both drug-like attributes (solubility, metabolic stability and safety) and maximal killing of the parasite in a shorter timeframe. Comparative appraisal of one preferred lead (**58**) in a chronic infection mouse model, monitored by highly sensitive bioluminescence imaging, provided the first definitive evidence of (partial) curative efficacy with this promising nitroimidazooxazine class.

Keywords: Chagas disease, pretomanid, library screening, *in vivo* efficacy, pharmacokinetics, bioluminescence imaging

Abbreviations

CD, Chagas disease; *T. cruzi*, *Trypanosoma cruzi*; HAT, human African trypanosomiasis; IPK, Institut Pasteur Korea; HLM, human liver microsomes; PK, pharmacokinetic; p.i., post-infection; MLM, mouse liver microsomes; STI, Swiss Tropical Institute; DIPEA, *N*,*N*-diisopropylethylamine; MEK, methyl ethyl ketone (2-butanone); NTR, nitroreductase; HRESIMS, high resolution electrospray ionisation mass spectrometry.

1. Introduction

Chagas disease (CD) or American trypanosomiasis is a neglected tropical disease that afflicts approximately 7 million people worldwide and claims at least 10,000 lives every year [1]. Once endemic almost exclusively to poor or rural areas of Latin America, CD has now spread into many high-income countries in Europe, North America, and the Western Pacific [2,3]. The causative parasite, *Trypanosoma cruzi* (*T. cruzi*), is transmitted primarily via the faeces of a blood-sucking triatomine insect known as the 'kissing bug', which commonly infests substandard housing; many animals also function as disease reservoirs [1-3]. Following infection, a one- to two-month acute illness develops, which is usually mild or asymptomatic, although it can be fatal in 5% of diagnosed cases due to the high parasitic burden. The host immune system then takes over, rendering even parasite detection extremely difficult [2,4]. Eventually, sometimes decades later, a chronic disease state can manifest in digestive or cardiac disorders, which may lead to malnutrition, progressive heart failure and sudden death [1,3]. However, in 2015, it was estimated that more than 80% of individuals affected by CD globally did not have access to diagnosis and specific treatment [5].

There is currently no vaccine for CD and just two drugs are available for therapy, benznidazole (**1**) and nifurtimox (**2**) (Fig. 1), both of which can induce serious adverse effects during dosing periods of 60-90 days [2,6,7]. Recent clinical trial failures with two azole drugs, posaconazole (**3**) and E1224 (**5**, a prodrug of ravuconazole **4**), have emptied the late-stage candidate pipeline, providing fresh impetus for the development of new assessment tools with superior predictivity [4,8-12]. One encouraging result is that the repositioned antimicrobial agent fexinidazole (**6**), a safe and effective newly approved drug for late-stage human African trypanosomiasis (HAT) [13], has shown curative activity potentially better than **1** in acute stage CD mouse models and equivalent to **1** in the chronic stage models, as revealed by highly sensitive bioluminescence imaging [14]. Although a phase II proof of concept clinical study of **6** was interrupted because of safety and tolerability issues at higher doses and longer treatment times, good efficacy against CD was observed at more tolerable doses; therefore, a second clinical trial has been initiated [15,16]. A close analogue of the HAT clinical candidate SCYX-7158 (**7**), oxaborole SCYX-6759 (**8**), also exhibited strong *in vivo* activity against CD but was not curative in the chronic model [17]. Amongst many novel lead molecules evaluated in mice [18-21], the most promising was proteasome inhibitor GNF6702 (**9**), which delivered an 88% cure rate for treating chronic infection when dosed twice daily for 20 days [22]. Nevertheless, a five day schedule using higher doses of **9** did not achieve *any* cures in the acute model [23], and a new article by Rao et al. [24] that compares **9** with a more recent analogue (for HAT) still provides no indication whether this pan-kinetoplastid drug candidate has progressed beyond preclinical toxicology. Hence, there remains a compelling need to discover new medicines for CD.

In CD research, successful target-based drug discovery has been hindered by the lack of well-validated targets [25]. Hence, phenotypic screening of various compound collections, seeking to exploit existing chemical matter, is still considered to be the most useful and cost-effective strategy to identify new leads or starting points [25,26]. Pretomanid (PA-824, **10**) is an orally active drug that was recently approved by the FDA to treat highly challenging cases of tuberculosis [27]. We have previously recounted that phenotypic screening (instigated by the Drugs for Neglected Diseases *initiative*, DND*i* [28]) of bicyclic nitroimidazole derivatives generated in our quest for an improved backup to **10** (with the TB Alliance [29]) led to the novel discovery of their potent antileishmanial activity [30,31]. Collaborative lead optimisation efforts with DND*i* in the very promising 7-substituted 2-nitroimidazooxazine class eventually culminated in the development of clinical candidate DNDI-0690 (**11**) [31], having comparable efficacy but greater safety than the original preclinical nominee, DNDI-VL-2098 (**12**) [30]. As

part of the early investigations (2010), a 900-member subset of the pretomanid analogue library above was counter-screened against intracellular Y strain *T. cruzi* amastigotes, using an image-based assay [8] (with 7 data points and 3-fold dilutions) run at the Institut Pasteur Korea (IPK). Following initial profiling of the best screening hits, we conducted some limited hit expansion work alongside our primary studies directed at leishmaniasis. Testing of these new compounds against *T. cruzi* pinpointed several that displayed submicromolar activity, some of which have been further assessed (e.g., for solubility, microsomal stability, *T. cruzi* CYP51 inhibition and maximal parasite killing in a 48 hour exposure assay). We now report the findings from our accumulated efforts to identify a suitable nitroimidazooxazine-based lead candidate for CD.

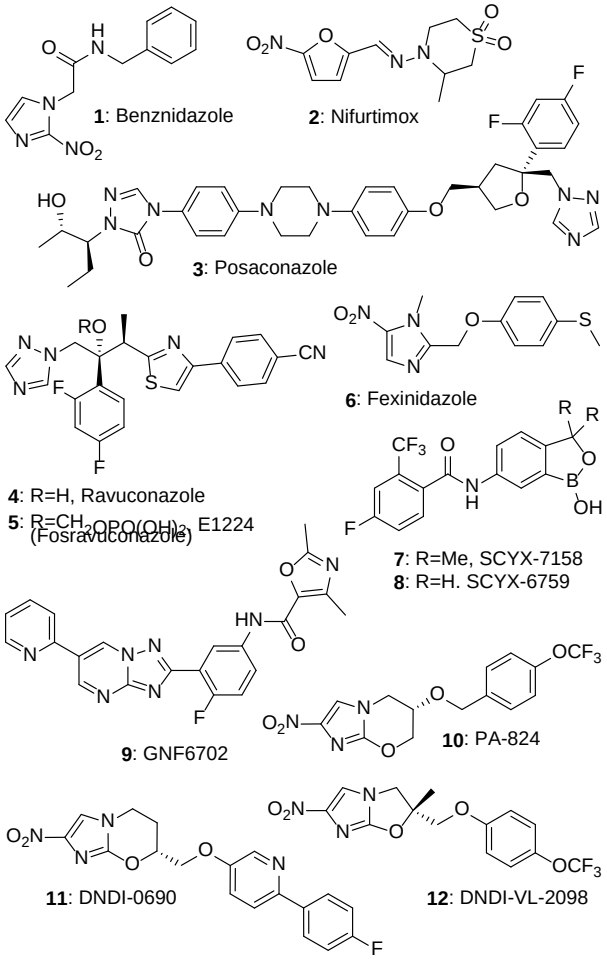

Fig. 1. Various antitrypanosomal, antitubercular, or antileishmanial agents.

2. Results and discussion

2.1 Initial examination of library screening hits

The structures and *in vitro* biological assay data for selected IPK screening hits (based mainly on % inhibition data) are summarised in Table 1. The IC_{50} and IC_{90} data against intracellular *T. cruzi* (transfected Tulahuen strain TcVI) or L6 host cells (rat skeletal myoblasts) were derived from replicate assays performed at Murdoch University [32], using fresh sample stock. Most of the hits provided submicromolar IC_{50} and IC_{90} values and displayed very low cytotoxicity, resulting in excellent selectivity indices (typically >200), but biphenyl analogues **16** and **21** [33] were much less effective. Unsurprisingly, these lipophilic compounds demonstrated very low aqueous solubilities. Five examples (**13**-**17**) [31,33-35] were also tested for stability in the presence of human liver microsomes (HLM). The first three showed more

rapid metabolism, consistent with known pharmacokinetic (PK) issues associated with the less stable 4-benzyloxybenzyl ether side chain (previously substantiated in both the nitroimidazooxazine and nitroimidazothiazine classes) [36,37]. This trend was further reinforced by measuring plasma concentrations of **13-17** in mice at time intervals of 0.5, 8 and 24 hours, following oral administration at 50 mg/kg. Only compounds **16** and **17** [31] gave plasma concentrations that were greater than their *in vitro* IC_{50} values at all time points (mean results at 24 hours were 9.1 and 0.78 µM, respectively; see the Supplementary data). These hits also showed little propensity to inhibit CYP3A4 (IC_{50} values >20 µM).

Table 1. Inhibitory potency, solubility and stability data for 12 screening hits against *T. cruzi*.

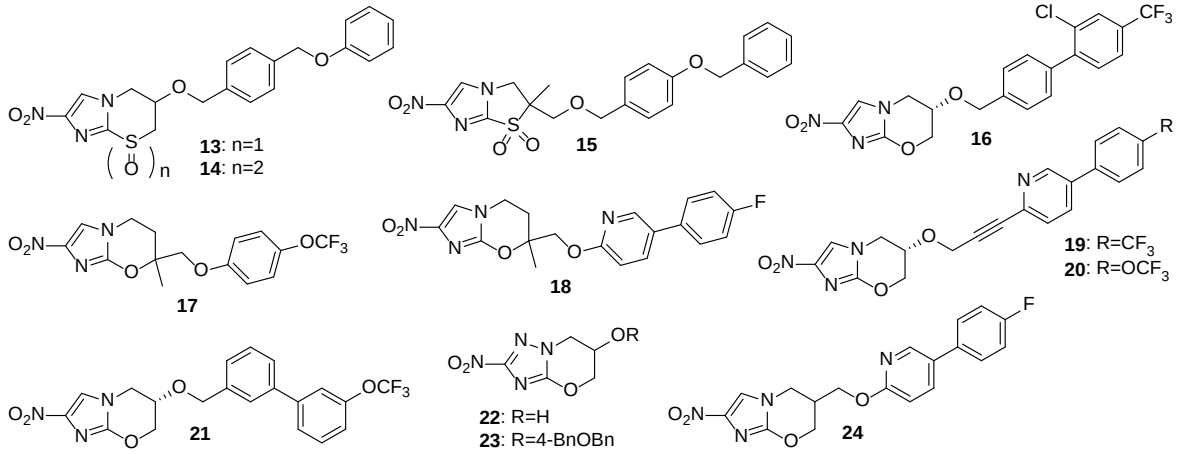

Compd	IPK Screen[a]	IC_{50} (µM)[b]		IC_{90} (µM)[b]	Selectivity	Solubility[d]	Stability[e]
	(% at x µg/mL)	*T. cruzi*	L6	*T. cruzi*	Index[c]	(µg/mL)	$t_{1/2}$ (min)
13	89% at 10	0.035	>100	0.089	>2857	0.44	156
14	95% at 10	0.28	>100	0.44	>357	0.13	103
15	59% at 3.3	0.083	>100	0.24	>1205	<0.1	25
16	94% at 10	3.7	34	8.0	9.2	0.48	>250
17	52% at 3.3	0.45	>100	0.93	>222	2.3	>250
18	50% at 3.3	0.31	>100	0.90	>323	0.69 (13)	ND
19	48% at 1.1	0.23	>100	0.59	>435	0.33 (6.8)	ND
20	44% at 0.37	0.32	>100	0.99	>313	0.49 (4.4)	>250
21	65% at 10	>10	13	>10	ND	ND	ND
22	58% at 1.1	1.6	>100	6.3	>63	8750	ND
23	(12% at 10)[f]	0.047	>100	0.13	>2128	0.18	ND
24	29% at 1.1	0.022	>100	0.19	>4545	1.1 (19)	ND

[a]Percentage inhibition of the growth of *T. cruzi* at the primary screen concentration (in µg/mL). [b]IC_{50} or IC_{90} values for inhibition of the growth of *T. cruzi* or for cytotoxicity toward L6 cells. Each value is the mean of ≥2 independent determinations. [c]Ratio of L6 to *T. cruzi* IC_{50} values. [d]Kinetic solubility in water, pH 7 (data in parentheses for 0.1 M HCl, pH 1; ND means not determined). [e]Half-life in human liver microsomes (data from a 60 min incubation). [f]Late inclusion based on promising data in an earlier *T. cruzi* assay run at the Swiss Tropical Institute.

*2.2 Evaluation of hit **17** in an acute infection mouse model of CD*

With these results in hand, a proof-of-concept *in vivo* efficacy study of **17** was initiated, using posaconazole (**3**) as a positive control. Briefly, female Swiss mice (5 per group) were infected intraperitoneally with 5 x 10^4 bloodstream form trypomastigotes of *T. cruzi* (Tulahuen strain). Oral dosing of compounds commenced on day 8 post-infection (p.i.), and continued once daily

for 20 days. Blood parasitemia was monitored during this period and mice having very low or undetectable parasite levels after the end of dosing and 10 days of rest were immunosuppressed via three rounds of treatment with cyclophosphamide (50 mg/kg once daily for 4 days, then 3 days of rest) to release any parasites that were being harboured in tissues [32]. In the absence of any therapy (vehicle only), all mice presented high parasitemia by day 12 p.i. In contrast, by day 28 p.i., treatment with **3** (20 mg/kg) had reduced parasite load below the detection limit in all five mice (Fig. 2a). However, after two rounds of immunosuppression (day 51 p.i.), parasite numbers had rebounded in three of the mice, and parasites were detected in the remaining two mice by PCR. Treatment with compound **17** (50 mg/kg) similarly decreased parasite load completely in 60% of mice, and greatly reduced parasitemia in the remainder (Fig. 2b), leading to 100% survival. Nevertheless, two rounds of immunosuppression subsequently led to the restoration of high parasite levels in all mice. Hence, while **17** showed promising efficacy in the acute phase of this study, like **3** (and oxaborole **8**, as reported earlier [17]), it did not ultimately deliver any complete cures. But success in treating this stringent model may require 24 hour plasma levels above the IC_{50} to be much higher than what was attained with **17** [32], implying the need for compounds with a superior PK profile and/or greater potency.

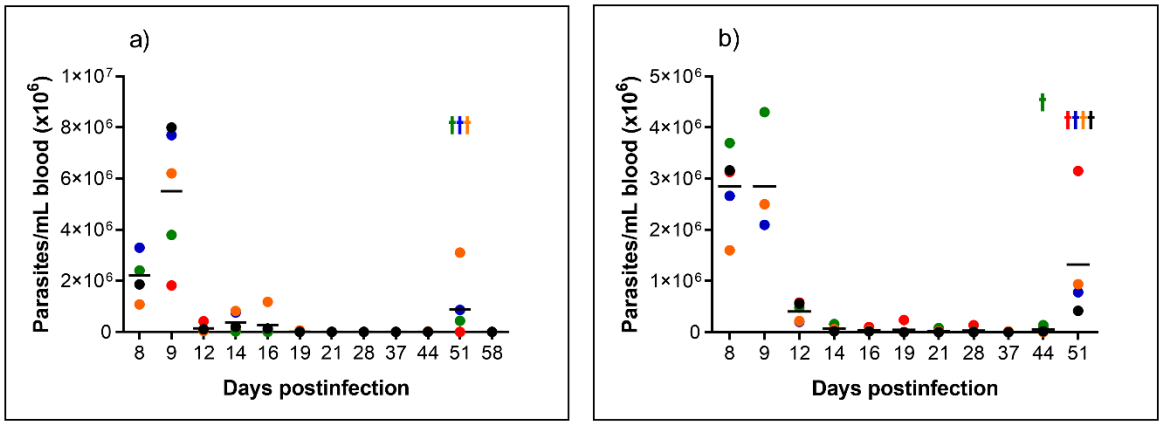

Fig. 2. Parasitemia levels in individual *T. cruzi*-infected mice over 20 days of oral treatment with a) **3** (20 mg/kg) or b) **17** (50 mg/kg) and then three 7-day cycles of immunosuppression.

2.3 Design and synthesis of new analogues

Looking at the remaining hits in Table 1, **18** [31] was not considered for *in vivo* study because it was rapidly metabolised by mouse liver microsomes (MLM; only 33% remained after a 30 min incubation [31]) and we held similar concerns about **23** [34] and **24** [38]. Therefore, at this point, we elected to perform some limited hit expansion work around **16**, **17**, **19** and **20** [36] to see if we could further improve potency and/or metabolic stability. In the mouse PK work above, the plasma concentration of **16** at 24 hours was 9.1 µM, 12-fold higher than that of **17**, but the potency of **16** was insufficient. Nevertheless, previous screening of an unsubstituted biphenyl analogue of **16** (**25**) [33] and its 6*R* enantiomer (*ent*-**25**) against intracellular *T. cruzi* (Tulahuen C2C4 strain) at the Swiss Tropical Institute (STI) had indicated that the latter was strongly preferred (22-fold; Fig. 3), suggesting that the enantiomers of **16**, **19** and **20** should be investigated. With **17**, we considered four alternative strategies for structural modification: (i) addition of a halogen atom to the 4-trifluoromethoxyphenyl ring (to block a potential site for metabolism); (ii) replacement of the ring oxygen by sulphur (and its oxide forms); (iii) replacement of the nitroimidazole ring by nitrotriazole; (iv) use of heterobiaryl side chains in the typically more potent 7*H* series. Proposals (ii) and (iii) were based on a comparison of **13** and **23** with 2-nitroimidazooxazine/thiazine counterparts **26** and **27** [34] (Fig. 3), whereas option (iv) was under concurrent study for visceral leishmaniasis [31].

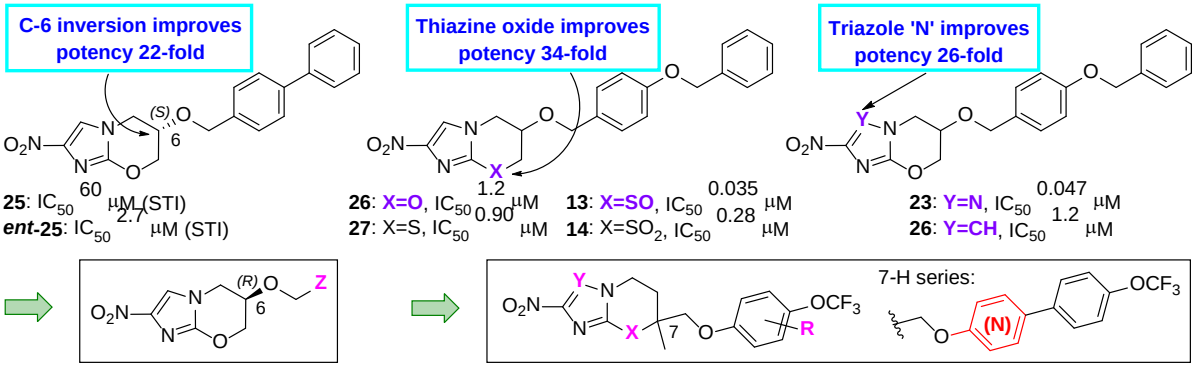

Fig. 3. Additional key data employed in the design of new targets.

The synthetic routes that were used to prepare these 13 new compounds are outlined below. The enantiomers of **16** and its 4-trifluoromethoxy congener **30** [33] were generated by Suzuki coupling reactions on the 4-bromobenzyl ether derivative of known 6*R* alcohol **28** [39], i.e. **29** (Scheme 1A). In similar fashion, phenylpyridine analogues **33** and *ent*-**33** were sourced from the 6*S* bromopyridine precursor **32** [40], or from 6*R* alcohol **28** and bromide **31** [40] (via *ent*-**32**), respectively. The construction of *ent*-**19** and *ent*-**20** involved successive Sonogashira and Suzuki reactions on key propargyl ether intermediate **36**, which was itself formed by alkylation of alcohol **28** with known bromide **34** [41], followed by desilylation (Scheme 1B).

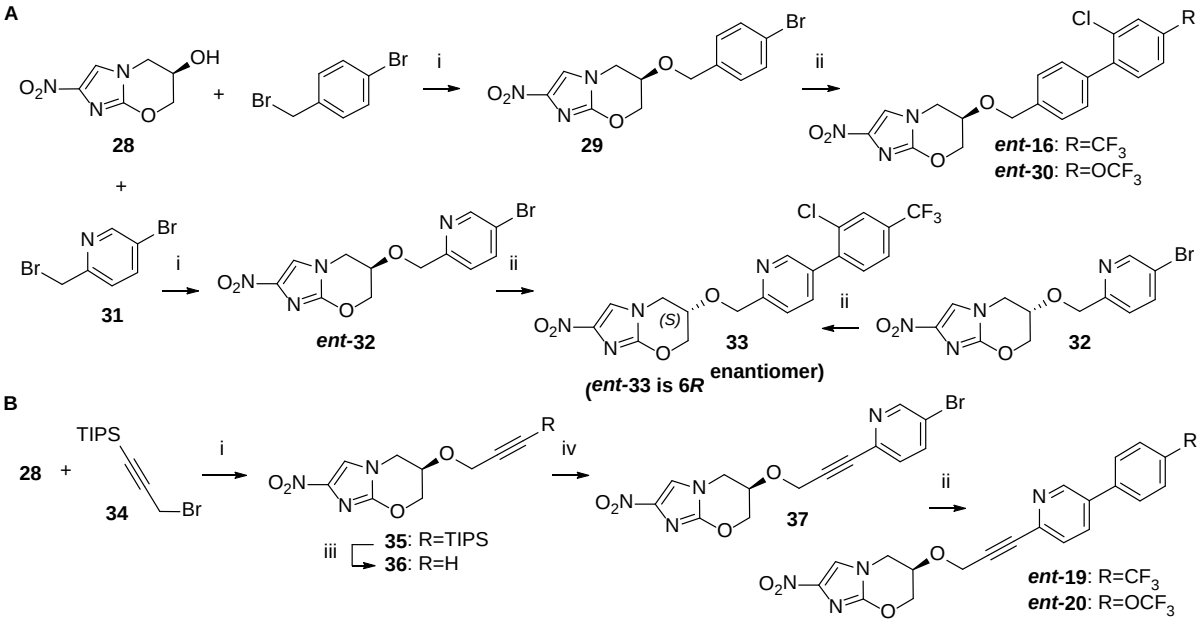

Scheme 1. Synthesis of new 6*R* enantiomers in the pretomanid class.
Reagents and conditions: (i) NaH, DMF, 0-20 °C, 1.8-3 h (87-95%); (ii) $ArB(OH)_2$, DMF, (toluene, EtOH), 2 M Na_2CO_3 or 2 M $KHCO_3$, $Pd(dppf)Cl_2$ under N_2, 70-89 °C, 1-16 h (34-81%); (iii) TBAF, THF, 0-6 °C, 2.5 h (81%); (iv) 5-bromo-2-iodopyridine, DIPEA, THF, DMF, CuI, $Pd(PPh_3)_2Cl_2$ under N_2, 20 °C, 24 h (82%).

Halide derivatives of **17** (**42**-**44**) were obtained from epoxide **38** (Scheme 2A) through ring opening with the required phenols (K_2CO_3, MEK, 80 °C), followed by sodium hydride-assisted ring closure of alcohol intermediates **39**-**41**, as reported for **17** [31]. Serendipitously, we discovered that treatment of **38** with thiourea on silica gel [42] readily afforded thiirane **45** (Scheme 2B) and that ring-opening of **45** with excess 4-(trifluoromethoxy)phenol (10 equiv) gave the desired 2-nitroimidazothiazine **46** directly, as the major product (27%). The low yield

in this latter case reflected the coproduction of polar decomposition material, possibly due to some competing reduction of the nitro group by the intermediate thiolate (at 80 °C). Buffered oxidations of **46** with *m*-CPBA (1.1 or 3.0 equiv) then selectively formed the monoxide (**47**) and dioxide (**48**) derivatives in high yield (88-96%). However, we postulated that the higher reactivity of 5-halo-3-nitrotriazoles toward nucleophiles would likely preclude the successful synthesis of triazole **56** using a similar epoxide-opening strategy. To circumvent this issue, the non-triazole portion of **56** was first assembled as iodide **53** (Scheme 2C), starting from the known epoxide **49** [43] [via successive epoxide ring opening with 4-(trifluoromethoxy)phenol, TBS-protection of the resulting tertiary hydroxyl group in **50**, hydrogenolysis to cleave the benzyl ether, and iodination of the obtained alcohol **52**]. Subsequently, iodide **53** was reacted with 5-bromo-3-nitro-1*H*-1,2,4-triazole (**54**) to produce the crude silyl ether **55**. Desilylation of the latter with TBAF then effected concomitant cyclization, giving the required nitrotriazolooxazine **56** in modest yield (28%). Competing hydrolysis of the activated bromide, leading to further side reactions, appeared to be a significant issue in the final two steps.

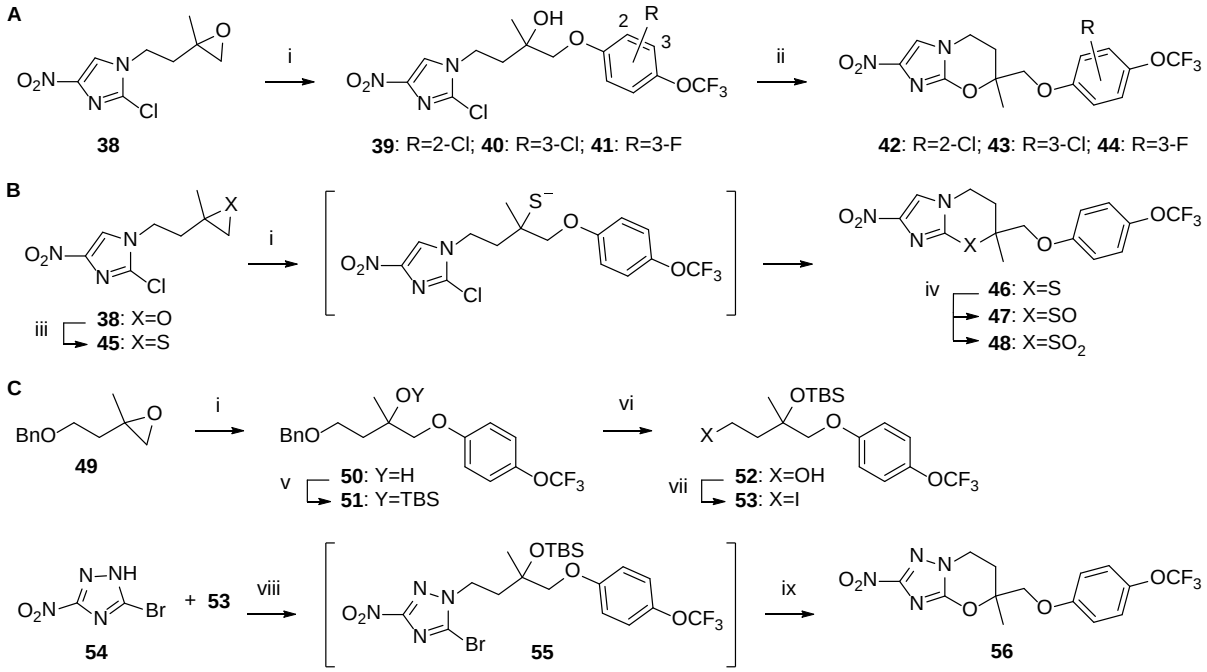

Scheme 2. Synthesis of new analogues in the 7-substituted oxazine/thiazine classes. Reagents and conditions: (i) ArOH, K_2CO_3, MEK, 80-83 °C, 10.5-108 h (**39**-**41**: 68-72%; **46**: 27%; **50**: 81%); (ii) NaH, DMF, 20 °C, 2.5-3 h (57-77%); (iii) thiourea on silica gel, CH_2Cl_2, 20 °C, 6.5 h (79%); (iv) *m*-CPBA, Na_2HPO_4, CH_2Cl_2, 20 °C, 17-53 h (88-96%); (v) TBSOTf, 2,6-lutidine, CH_2Cl_2, 0-20 °C, 66 h (95%); (vi) H_2, Pd/C, EtOH, EtOAc, 20 °C, 42 h (100%); (vii) I_2, PPh_3, imidazole, CH_2Cl_2, 20 °C, 39 h (96%); (viii) K_2CO_3, DMF, 73 °C, 61 h (45%); (ix) TBAF, THF, 0-20 °C, 24 h (28%).

2.4 Initial in vitro assessment of new and known analogues

The biological effects of our initial hit expansion work around **16** are recorded in Table 2. While close analogues **30** and **33** did not show better activity than **16**, the 6*R* enantiomers of all three compounds (*ent*-**16**, *ent*-**30**, and *ent*-**33**) were an order of magnitude more growth inhibitory against *T. cruzi*, having potencies comparable to that of the known [44] 6*R* enantiomer of pretomanid (*ent*-**10**). Both 6*S* and 6*R* forms were similarly cytotoxic toward L6 host cells, so this increased activity for the latter derivatives translated into greatly improved selectivity indices (values >100, compared to only 3-12 for **16**, **30**, and **33**). Continued

optimisation of the phenylpyridine class exemplified by *ent*-**33** as antileishmanial agents (counter-screening against *T. cruzi*) led to compounds with very high potencies (e.g., **57**: IC_{50} 0.049 μM), but these were metabolised much more rapidly (half-lives of ~30 min in HLM; Table 3) and were found to be strong inhibitors of the hERG channel (e.g., **57**: IC_{50} 0.81 μM *cf.* >30 μM for **16**) [45]. Amongst monoaryl counterparts, *ent*-**10** displayed good solubility but was reportedly cleared faster than **10** *in vivo*, such that plasma levels were undetectable by 24 hours [44]. However, close analogue **58** was identified as a potential lead for CD, given its good *in vitro* activity (IC_{90} 1.0 μM), acceptable aqueous solubility (12 μg/mL), and excellent rodent PK and safety profile [45].

Table 2. Inhibitory potency data for pretomanid series hits and new analogues.

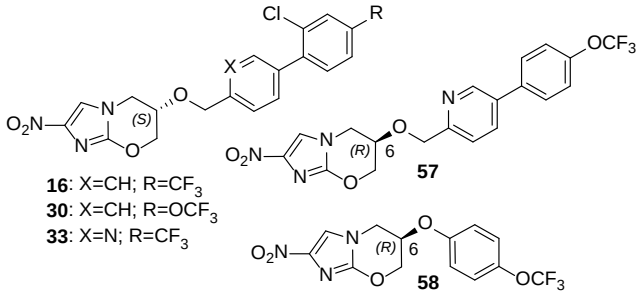

Compd	IC_{50} (μM)[a]		IC_{90} (μM)[a]	Selectivity
	T. cruzi	L6	*T. cruzi*	Index[b]
16	3.7	34	8.0	9.2
30	5.7	19	>10	3.3
33	4.8	57	>10	12
ent-**10**	0.30	72	1.4	240
ent-**16**	0.25	29	0.71	116
ent-**30**	0.24	25	1.1	104
ent-**33**	0.67	50	2.9	75
57	0.049	51	0.31	1041
58	0.40	>100	1.0	>250

[a]IC_{50} or IC_{90} values for inhibition of the growth of *T. cruzi* or for cytotoxicity toward L6 host cells. Each value is the mean of ≥2 independent determinations. [b]Ratio of L6 to *T. cruzi* IC_{50} values.

In the 7-substituted 2-nitroimidazooxazine class (Table 4), addition of a chlorine or fluorine atom to the 4-trifluoromethoxyphenyl ring of **17** (**42**-**44**) seemed to be fairly well tolerated, but this modification unexpectedly led to more rapid rates of metabolism by HLM and MLM (Table 3). Furthermore, exchange of the oxazine ring of **17** for thiazine and its oxides (**46**-**48**) did not furnish the same enhancement in potency observed in the parent 6-substituted series (*cf.* **13** and **14** vs **26**). Therefore, we switched our attention to heterobiaryl side chains in the more active 7*H* series [31] (Table 5). Here, the incorporation of 2,6-pyrimidine or 2-pyridine as the first ring (**61** and **63**) [31] was particularly efficacious (IC_{90}s 0.18-0.33 μM) but the compounds were only sparingly soluble (Table 3). More extensive optimisation of this biaryl class for visceral leishmaniasis led to the identification of *rac*-**11** as a lead with good *T. cruzi* activity (similar to its 4-trifluoromethoxy counterpart **64**), but the standout new hit for CD was **65** [31]. This compound had superb potency (IC_{90} 0.044 μM) and low cytotoxicity (IC_{50} >100 μM), giving a very high selectivity index (>5556); it also demonstrated solubility comparable to *rac*-**11** (at pH 7) and excellent MLM stability (90% parent after 1 h; Table 3).

Table 3. Aqueous solubility, microsomal stability, and hERG data for selected compounds.

Compd	Aq. Solubility[a] (μg/mL)		Microsomes[b] (% remaining at 1 h)		hERG IC_{50}
	pH 7	pH 1	Human	Mouse	(μM)
ent-**10**[c]	18		92	86	
rac-**11**[d]	0.32	164	44	34	>30
rac-**12**[e]	3.6				5.6
16[f]	0.48		92	93	>30
ent-**16**	<0.1		76	83	
17[d]	2.3		58	50	3.8
19[g]	0.33	6.8			
ent-**19**	0.68	7.6	58	76	
20[g]	0.49	4.4	89	86	
ent-**20**	<0.1	3.0	68	74	
ent-**30**	<0.1		85	76	
ent-**33**	1.0	299			
42	0.61		6.4	9.1	
43	0.50		11	8.8	
44	0.95		26	23	
48	1.1		88	76	
56	9.5[h]		91	92	
57[c]	3.0	1040	27	36	0.81
58[c]	12		81	79	>30
59[d]	<0.1				
60[d]	0.46				
61[d]	<0.1				
62[d]	<0.1				
63[d]	<0.1	0.9			
64[d]	0.15	138	53	41	
65[d]	0.36		72	90	
70[c]	0.85		80	76	

[a]Kinetic solubility in water (pH 7) or 0.1 M HCl (pH 1), determined by HPLC. [b]Pooled human or CD-1 mouse liver microsomes. [c]Ref. 45. [d]Ref. 31. [e]Ref. 30. [f]Ref. 33. [g]Ref. 36. [h]1% DMSO.

Table 4. Inhibitory potency data for new analogues of 7-substituted oxazine hit **17**.

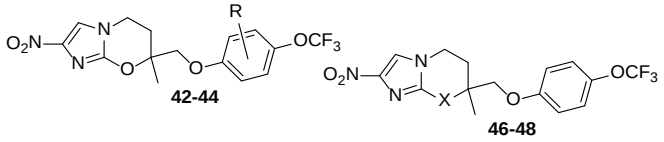

Compd	R or X	IC_{50} (μM)[a]		IC_{90} (μM)[a]	Selectivity Index[b]
		T. cruzi	L6		
17		0.45	>100	0.93	>222
42	2-Cl	0.46	>100	1.3	>217
43	3-Cl	0.31	53	6.5	171
44	3-F	0.56	68	1.9	121
46	S	1.1	>100	2.6	>91
47	SO	1.6	73	3.7	46
48	SO_2	0.70	>100	1.6	>143

[a,b]As for Table 2.

Table 5. Inhibitory potency data for various known 7-substituted oxazine biaryl derivatives.

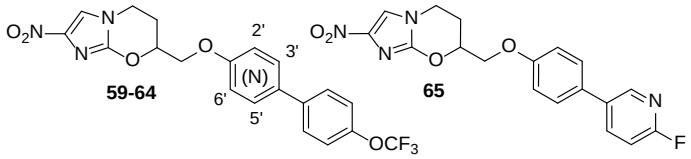

Compd	Aza	IC_{50} (μM)[a]		IC_{90} (μM)[a]	Selectivity
		T. cruzi	L6	*T. cruzi*	Index[b]
59	2′,3′	0.38	42	0.96	111
60	2′,5′	0.21	>100	6.7	>476
61	2′,6′	0.053	19	0.33	358
62	3′,5′	0.33	70	0.96	212
63	2′	0.040	>100	0.18	>2500
64	3′	0.24	>100	0.99	>417
rac-**11**		0.17	>100	0.56	>588
65		0.018	>100	0.044	>5556

[a,b]As for Table 2.

2.5 Further in vitro assessment of various new and known leads

Selected compounds from this work and our previous studies [30,31,45] (Table 6) were then further profiled *in vitro* at the University of Dundee and Griffith University to respectively test for inhibition of sterol 14α-demethylase (CYP51) in *T. cruzi* (the commonly targeted mechanism of action of azoles **3**-**5** that we wished to avoid, due to the failure of such drugs in CD clinical trials) [46] and for the ability to achieve 100% trypanocidal activity against *T. cruzi* (Tulahuen strain) amastigotes in a shorter 48 (vs 96) hour assay [47] (a distinguishing feature of **1** and **2** over **3** and other CD drug candidates [8]). In the initially studied (for leishmaniasis) imidazooxazole class [30], both the des-nitro analogue **66** and 5-bromo derivative **67** showed submicromolar inhibition of CYP51 (IC_{50}s 0.16 and 0.53 μM, respectively), possibly accounting (at least in part) for their unexpected activities against *T. cruzi*. However, some conversion of the photosensitive **67** to **66** prior to or during this assay could not be excluded because 5-thioether **68** displayed no inhibition of CYP51. Importantly, nitro derivatives across all compound classes were generally inactive against CYP51 (IC_{50}s >10 μM), implying a mechanism of action different to that of azoles **3**-**5**.

Continued examination of oxazole-based classes revealed that for the two more potent nitro compounds (*rac*-**12** and **69**: IC_{90}s 2.3 and 2.1 μM, respectively) there were substantial differences in their maximal inhibitory activities against *T. cruzi* in this shorter (48 h) assay, with triazole **69** (96%) being much more effective than its imidazole counterpart *rac*-**12** (68%). Intriguingly, the tuberculosis drug delamanid (a 2-nitroimidazooxazole) was similarly reported to be a slow cidal inhibitor of *T. cruzi in vitro* (a characteristic also shown by CYP51 inhibitors [8]), and this was postulated to be a predictive factor for its failure to demonstrate *in vivo* efficacy in a CD mouse model [48]. The mechanism of action of delamanid for CD has not been determined but a novel nitroreductase (NTR2) in *Leishmania* (rather than the previously identified type I nitroreductase NTR1) was shown to be responsible for mediating its antileishmanial effects [49]. The involvement of an analogous new target in CD would be consistent with evidence from studies in HAT revealing a lack of cross resistance between pretomanid (**10**) and nifurtimox (**2**) [50], and that a more potent 6-amino-linked analogue of **10** was not activated by NTR1 [51]**.** Nonetheless, a nitroreductase-based mechanism would not explain the inhibitory activity of 5-thiomethyl derivative **68**.

Table 6. Further *in vitro* data on various leads (*T. cruzi* IC_{50}s above table from refs 30 and 45).

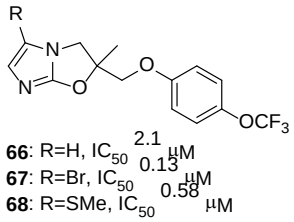

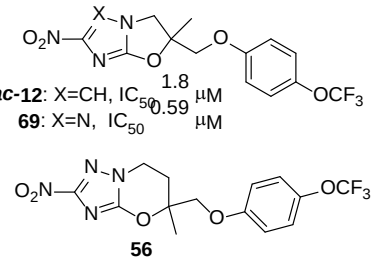

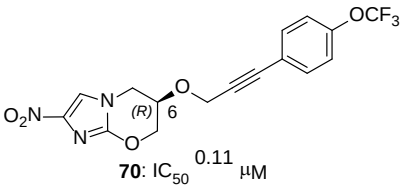

Compd	IC_{50} (µM)[a]			IC_{90} (µM)[a]	Selectivity	Maximum	Hill
	T. cruzi	3T3	CYP51	*T. cruzi*	Index[b]	Activity (%)	Slope
1	12	>127	>10[c]	37	>11	101	2.4
2	2.1	>127	>10[c]	4.6	>60	99	2.7
3	0.0012	>1	0.052	0.0049	>833	85	1.8
			Pretomanid class				
ent-**10**	0.89	>37	>10	5.9	>42	94	1.2
ent-**16**	0.28	>37	7.6	0.41	>132	100	6.3
19	0.51	>37	>10	1.7	>73	97	1.9
ent-**19**	0.27	>37	>10	1.7	>137	95	1.2
20	0.73	>37	>10	1.0	>51	99	7.0
ent-**20**	0.67	>37	>10	2.2	>55	94	1.8
ent-**30**	0.57	>37	>10	1.0	>65	99	4.6
57	0.39	>73	>10	2.6	>187	80	1.2
58	1.2	>73	>10	1.7	>61	99	12
70	0.19	>37	>10	0.44	>195	99	2.8
			7-Substituted oxazine/thiazine classes				
17	0.17	>37	>10	1.0	>218	100	1.3
48	1.3	>37	>10	3.0	>28	101	2.6
56	0.22	>37	>10	0.85	>168	96	1.7
64	1.0	>73	>10	1.5	>73	100	5.6
65	0.074	>37	>10	0.33	>500	98	1.5
			Imidazooxazole/Triazolooxazole classes				
rac-**12**	0.95	>73	>10	2.3	>77	68	3.4
66	4.7	>73	0.16	10	>16	80	2.9
67	1.7	>73	0.53	4.1	>43	87	6.8
68	2.0	>73	>10	16	>37	93	1.1
69	0.72	>73	>10	2.1	>101	96	2.0

[a]IC_{50} or IC_{90} values for inhibition of the growth of *T. cruzi* (48 hour assay), for cytotoxicity toward 3T3 cells, or for inhibition of *T. cruzi* CYP51. Each value (except the single test CYP51 data) is the mean of 2 independent determinations (for standard deviations, see the Supplementary data). [b]Ratio of 3T3 to *T. cruzi* IC_{50} values. [c]Data from ref 11.

In the pretomanid class, several compounds (*ent*-**16**, **20**, *ent*-**30**, **58** and **70**) showed maximal inhibitory activities of 99-100%, of which *ent*-**16** and arylpropargyl ether **70** were the most potent (IC_{90}s 0.41 and 0.44 µM, respectively). However, *ent*-**10**, **19**, and the 6*R* enantiomers of **19** and **20** were somewhat less efficacious (94-97% inhibition) and phenylpyridine analogue **57** was markedly inferior (80%). For this class, higher maximal activity seemed to be associated with steeper dose-response curves (see Fig. 4 below and additional Figures S1 and S2 in the Supplementary data). Nevertheless, this tendency was not observed in the 7-substituted oxazine/thiazine classes (or the oxazole-based classes), where early lead **17**,

thiazine dioxide **48** and phenylpyridine **64** each provided 100% inhibition, but two more potent analogues, triazole **56** and phenylpyridine **65** (IC_{90}s 0.85 and 0.33 µM, respectively), gave slightly lower maximal effects (96-98%). The result with triazole **56** was rather unexpected in light of the reverse trend for oxazole analogues *rac*-**12** and **69**, and also unfortunate, given its better solubility and microsomal stability profile. Overall, based on the data in Table 6, the most promising candidates for further assessment as CD leads were the 2-nitroimidazooxazine derivatives *ent*-**16**, **20**, *ent*-**30**, **58**, **64** and **70.**

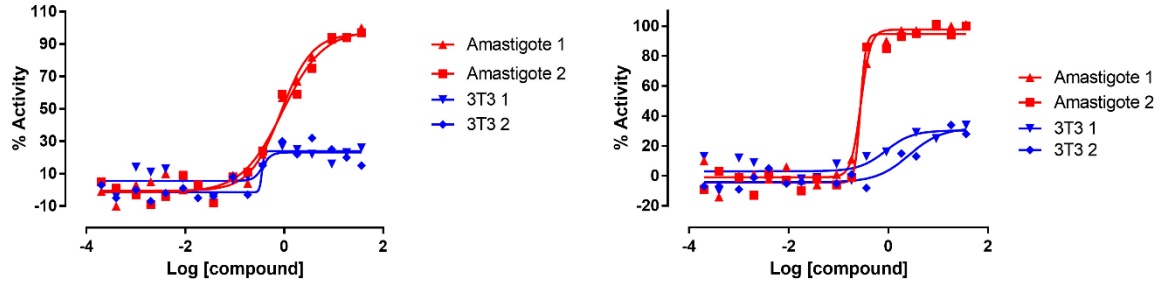

Fig. 4. Duplicate dose-response curves depicting percentage trypanocidal activity against *T. cruzi* or percentage cytotoxicity toward 3T3 cells for *ent*-**10** (left) and *ent*-**16** (right).

*2.6 Assessment of lead **58** in a chronic infection mouse model of CD*

To conclude this current investigation, we elected to evaluate **58** alongside **1**, **2** and **6** in the chronic *T. cruzi* infection mouse model, monitoring the parasite burden using highly sensitive bioluminescence imaging [52] (Fig. 5). The choice of **58** (DNDI-8219, a backup lead candidate for visceral leishmaniasis [45]) for a second proof-of-concept *in vivo* efficacy study was based on its better solubility (12 µg/mL) and high 24 hour exposure in mice (see Figure S4 in the Supplementary data; the mean plasma concentration of **58** at 24 hours was 11 µM), together with its strong *in vitro* activity and suitable safety profile. In this experiment, female BALB/c mice (five per group) were infected intraperitoneally with 10^3 bioluminescent bloodstream trypomastigotes of CL Brener *T. cruzi* strain. Commencing on day 114 p.i., these mice were orally dosed with test compounds at 50 or 100 mg/kg once daily for five days. Apart from a vehicle-related effect in one case (discussed below), dosing regimens were well tolerated, and body weight changes for the mice in this experiment were well within normal thresholds.

After the end of dosing and a 17 day rest period, treated mice were immunosuppressed using cyclophosphamide (200 mg/kg), administered intraperitoneally on days 135, 139 and 143 p.i. All untreated mice were found to be bioluminescence positive at each time point. On day 149 p.i., imaging of mice treated with benznidazole (**1**) or fexinidazole (**6**) (100 mg/kg in 5% DMSO/HPMC-SV) indicated that all mice were bioluminescence negative, so these were designated as cured; similarly, 4 out of 5 mice treated with nifurtimox (**2**) (100 mg/kg in the same vehicle) were cured (see Figure S5 in the Supplementary data for imaging results on **1**, **2**, **6** and vehicle). In the case of **58** (dosed at only 50 mg/kg in PEG400), all mice appeared to be bioluminescence negative at day 143 p.i., but at day 149, only mouse #5 remained negative and was considered cured (Fig. 5A). An *ex vivo* analysis revealed that the internal organs of mouse #4 were also bioluminescence negative, but a small positive signal was detected in the mouth/nasal region, while mouse #2 displayed bioluminescent foci in the small intestine and caecum (Fig. 5C). However, it should be noted that the vehicle employed for dosing of **58** (200 µL of PEG400) induced daily diarrhoea in all treated mice, which may have had a detrimental effect on the efficacy outcome. This is because PEG400 is known to markedly accelerate liquid transit through the small intestine, the primary site of drug absorption in the gastrointestinal tract [53]; shorter residence times would result in less drug absorption and suboptimal efficacy.

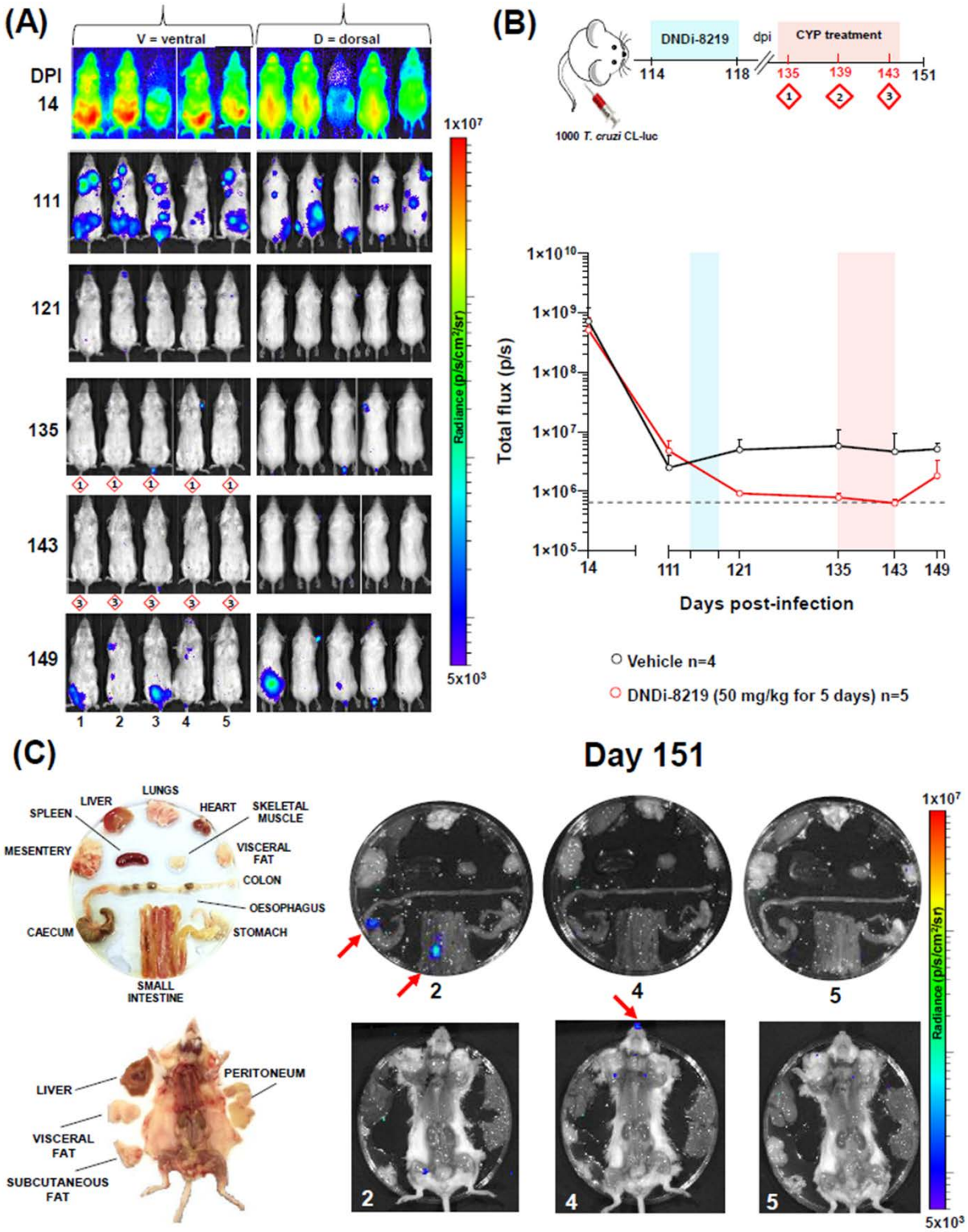

Fig. 5. *In vivo* evaluation of **58** (DNDI-8219) as a treatment for chronic stage *T. cruzi* infection. **(A)** Ventral (V) and dorsal (D) images of each mouse are shown at various days post-infection (DPI). **(B)** Experimental design and inset graph showing average total body bioluminescence (sum of ventral and dorsal images) for mice treated with **58** or vehicle only. The pale blue bar indicates timing of treatment and the pink bar highlights the cyclophosphamide treatment period. The dashed grey line indicates background levels for naïve BALB/c mice. **(C)** *Ex vivo* assessment of bioluminescence for mice #2, #4 and #5 at day 151 p.i. Heat-maps are on log10 scales and indicate the intensity of bioluminescence from low (blue) to high (red).

The measured thermodynamic solubility of **58** in PEG400 (21 mg/mL) was more than four times the concentration employed for this dosing experiment (5 mg/mL), suggesting that reduction of the dose volume, alternative formulation, or extension of the treatment period beyond 5 days might facilitate an improved therapeutic outcome for this promising lead compound in future studies.

3. Conclusions

To summarise, in response to a dire need for new medications to treat CD, an early-stage chemical library of antitubercular bicyclic nitroimidazole derivatives was screened against *T. cruzi*, and a selection of 12 hits was profiled *in vitro*. Mouse pharmacokinetic data generated on five on these directed our initial focus toward the evaluation of **17** in a CD mouse model, albeit, promising efficacy in the acute phase was overturned after immunosuppression with cyclophosphamide, implying the need for greater 24 hour plasma levels or better potency. Within limited hit expansion studies, highly novel nitrotriazole and nitroimidazothiazine dioxide analogues of **17** provided improved microsomal stability, while more active 6*R* enantiomers of several 6*S* pretomanid derivatives were also earmarked as promising leads for follow-up. Further assessment of these and some additional hits derived from our leishmaniasis studies in a 48 hour *T. cruzi* growth inhibition assay pinpointed a set of six 2-nitroimidazooxazine derivatives that provided superior results (maximal activity of 99-100% and IC_{90} values below 2 μM). Of these, **58** (DNDI-8219) possessed the best drug-like attributes (in terms of solubility, metabolic stability and safety) and proved to be effective in completely curing one of five mice in a chronic infection mouse model, as well as markedly reducing parasite burdens in two other mice. Given the short five-day treatment schedule and less ideal formulation administered in that experiment, this result is considered to be very encouraging and provides good rationale for future studies of this dual antileishmanial/antitrypanosomal 2-nitroimidazooxazine class.

4. Experimental section

4.1 General information

Elemental analyses were performed by the Campbell Microanalytical Laboratory, University of Otago, Dunedin, New Zealand. Melting points were determined using an Electrothermal IA9100 melting point apparatus and are as read. NMR spectra were measured on a Bruker Avance 400 spectrometer at 400 MHz for ^{1}H and 100 MHz for ^{13}C and were referenced to Me_4Si or solvent resonances. Chemical shifts and coupling constants were recorded in units of ppm and hertz, respectively. High-resolution electrospray ionisation (HRESIMS) mass spectra were determined on a Bruker micrOTOF-Q II mass spectrometer or an Agilent 6530 Q-TOF mass spectrometer coupled to an Agilent 1200 series HPLC system. Column chromatography was performed on silica gel (Merck 230-400 mesh). Thin-layer chromatography was carried out on aluminium-backed silica gel plates (Merck 60 F_{254}), with visualization of components by UV light (254 nm), I_2, or $KMnO_4$ staining. Tested compounds (including batches screened *in vivo*) were ≥95% pure, as determined by elemental analysis and/or by HPLC conducted on an Agilent 1100 system with diode array detection, using a 150 mm x 3.2 mm Altima 5 μm reversed phase C8 or C18 column. Elemental analyses indicated by the symbols of the elements were within ± 0.4% of the theoretical values.

*4.2 General procedure for the syntheses of aryl bromides **29**, **ent-32**, and **37** (via **35**)*

Sodium hydride (60% in mineral oil, unwashed, 1.4-1.6 equiv) was added to a mixture of (6*R*)-2-nitro-6,7-dihydro-5*H*-imidazo[2,1-*b*][1,3]oxazin-6-ol [39] (**28**) (1.0 equiv) and the appropriate halide (1.5 equiv) in anhydrous DMF (2 mL/100 mg of alcohol) under N_2 at 0 °C. The mixture was immediately degassed and resealed under N_2 and then stirred at 20 °C for 3 h. The resulting mixture was rapidly cooled (CO_2/acetone), quenched with ice/aqueous $NaHCO_3$ (5 mL), added to brine (50 mL), and extracted with CH_2Cl_2 (5 x 50 mL). The combined extracts were evaporated to dryness under reduced pressure (at 30 °C) and the residue was chromatographed on silica gel (0-0.75% MeOH/CH_2Cl_2 or 0-2% EtOAc/CH_2Cl_2) and then crystallized to afford the required products.

*4.2.1 (6R)-6-[(4-Bromobenzyl)oxy]-2-nitro-6,7-dihydro-5H-imidazo[2,1-b][1,3]oxazine (**29**)*
The title compound was obtained from alcohol **28** and 4-bromobenzyl bromide. Cream solid (89% yield): mp (MeOH/CH_2Cl_2/hexane) 190-191 °C; ^{1}H NMR [$(CD_3)_2SO$] δ 8.03 (s, 1 H), 7.54 (br d, *J* = 8.4 Hz, 2 H), 7.27 (br d, *J* = 8.4 Hz, 2 H), 4.66 (dt, *J* = 12.0, 2.2 Hz, 1 H), 4.64 (d, *J* = 12.2 Hz, 1 H), 4.60 (d, *J* = 12.2 Hz, 1 H), 4.46 (br d, *J* = 12.0 Hz, 1 H), 4.30-4.19 (m, 3 H). Anal. ($C_{13}H_{12}BrN_3O_4$) C, H, N.

*4.2.2 (6R)-6-[(5-Bromopyridin-2-yl)methoxy]-2-nitro-6,7-dihydro-5H-imidazo[2,1-b][1,3]oxazine (ent-**32**)*
The title compound was obtained from alcohol **28** and 5-bromo-2-(bromomethyl)pyridine [40] (**31**) (1.2 equiv), using the above procedure for 135 min. Pale yellow solid (95% yield): mp (MeOH/CH_2Cl_2/hexane) 171-173 °C; ^{1}H NMR [$(CD_3)_2SO$] δ 8.65 (br d, *J* = 2.4 Hz, 1 H), 8.05 (dd, *J* = 8.4, 2.4 Hz, 1 H), 8.04 (s, 1 H), 7.35 (br d, *J* = 8.4 Hz, 1 H), 4.76-4.66 (m, 3 H), 4.49 (br d, *J* = 11.8 Hz, 1 H), 4.35-4.28 (m, 2 H), 4.24 (dd, *J* = 13.7, 3.5 Hz, 1 H). Anal. ($C_{12}H_{11}BrN_4O_4$) C, H, N.

*4.2.3 Synthesis of bromide **37***

*4.2.3.1 (6R)-2-Nitro-6-{[3-(triisopropylsilyl)prop-2-yn-1-yl]oxy}-6,7-dihydro-5H-imidazo[2,1-b][1,3]oxazine (**35**)*
The title compound was obtained from alcohol **28** and (3-bromoprop-1-yn-1-yl)triisopropylsilane [41] (**34**), using the above procedure at 0-5 °C for 110 min. Cream solid (87% yield): mp (CH_2Cl_2/pentane) 89-91 °C; ^{1}H NMR ($CDCl_3$) δ 7.41 (s, 1 H), 4.66-4.60 (m, 1 H), 4.43-4.33 (m, 4 H), 4.26-4.15 (m, 2 H), 1.08 (s, 21 H); HRESIMS calcd for $C_{18}H_{30}N_3O_4Si$ *m*/*z* $[M + H]^+$ 380.2000, found 380.2016.

*4.2.3.2 (6R)-2-Nitro-6-[(prop-2-yn-1-yl)oxy]-6,7-dihydro-5H-imidazo[2,1-b][1,3]oxazine (**36**)*
A stirred solution of silyl ether **35** (1.79 g, 4.72 mmol) in anhydrous distilled THF (40 mL) under N_2 at 0 °C was treated with TBAF (5.05 mL of a 1 M solution in THF, 5.05 mmol). The mixture was stirred at 0-6 °C for 2.5 h, then diluted with ice/aqueous $NaHCO_3$ (100 mL) and extracted with CH_2Cl_2 (5 x 100 mL). The combined extracts were evaporated to dryness under reduced pressure (at 30 °C) and the residue was chromatographed on silica gel (25-75% EtOAc/petroleum ether) to afford the title compound. Pale yellow solid (0.85 g, 81% yield): mp (Et_2O/pentane) 81-83 °C; ^{1}H NMR ($CDCl_3$) δ 7.42 (s, 1 H), 4.63 (ddd, *J* = 12.5, 3.8, 2.1 Hz, 1 H), 4.42-4.33 (m, 3 H), 4.32 (dd, *J* = 16.6, 2.6 Hz, 1 H), 4.25 (dd, *J* = 13.0, 3.7 Hz, 1 H), 4.18 (dt, *J* = 12.9, 2.4 Hz, 1 H), 2.56 (t, *J* = 2.4 Hz, 1 H); HRESIMS calcd for $C_9H_9N_3NaO_4$ *m*/*z* $[M + Na]^+$ 246.0485, found 246.0484.

*4.2.3.3 (6R)-6-{[3-(5-Bromopyridin-2-yl)prop-2-yn-1-yl]oxy}-2-nitro-6,7-dihydro-5H-imidazo[2,1-b][1,3]oxazine (**37**)*

A mixture of alkyne **36** (351 mg, 1.57 mmol), 5-bromo-2-iodopyridine (891 mg, 3.14 mmol), bis(triphenylphosphine)palladium(II) dichloride (73.7 mg, 0.105 mmol), and copper(I) iodide (23.9 mg, 0.125 mmol) in anhydrous DMF (9 mL), anhydrous distilled THF (7 mL) and DIPEA (1.80 mL, 10.3 mmol) was degassed for 10 min (vacuum pump) and then N_2 was added. The mixture was stirred at 20 °C for 24 h and then diluted with ice/aqueous $NaHCO_3$ (100 mL) and extracted with CH_2Cl_2 (5 x 80 mL). The combined extracts were evaporated to dryness under reduced pressure (at 30 °C) and the residue was chromatographed on silica gel (0-1% MeOH/CH_2Cl_2) to afford the title compound. Light yellow solid (488 mg, 82% yield): mp (MeOH/CH_2Cl_2/hexane) 190-191 °C; ^{1}H NMR [$(CD_3)_2SO$] δ 8.71 (br d, *J* = 2.4 Hz, 1 H), 8.10 (dd, *J* = 8.4, 2.4 Hz, 1 H), 8.04 (s, 1 H), 7.54 (br d, *J* = 8.4 Hz, 1 H), 4.67 (dt, *J* = 12.1, 2.5 Hz, 1 H), 4.62 (s, 2 H), 4.49 (br d, *J* = 12.0 Hz, 1 H), 4.41-4.36 (m, 1 H), 4.31 (dt, *J* = 13.7, 2.0 Hz, 1 H), 4.25 (dd, *J* = 13.6, 3.2 Hz, 1 H); HRESIMS calcd for $C_{14}H_{12}BrN_4O_4$ *m/z* $[M + H]^+$ 381.0018, 379.0036, found 381.0037, 379.0055.

*4.3 General procedure for the syntheses of ent-**16**, ent-**30**, **33** and ent-**33***

A mixture of the bromide (**29**, **32**, or *ent*-**32**, 400 mg, 1.0 equiv), arylboronic acid (1.7 equiv) and [1,1′-bis(diphenylphosphino)ferrocene]dichloropalladium(II) (0.07 equiv) in DMF (6 mL) and aqueous $KHCO_3$ (2 mL of 2 M, 4.0 mmol) was degassed, and then N_2 was added. The resulting mixture was stirred at 75 °C for 4 h and then cooled, diluted with brine (100 mL), and extracted with CH_2Cl_2 (3 x 100 mL). The extracts were evaporated to dryness under reduced pressure and the residue was chromatographed on silica gel (0-2% MeOH/CH_2Cl_2) and then triturated in CH_2Cl_2/hexane to afford the required products.

*4.3.1 (6R)-6-{[2'-Chloro-4'-(trifluoromethyl)[1,1'-biphenyl]-4-yl]methoxy}-2-nitro-6,7-dihydro-5H-imidazo[2,1-b][1,3]oxazine (ent-**16**)*

The title compound was obtained from bromide **29** and [2-chloro-4-(trifluoromethyl)phenyl]boronic acid. Cream solid (81% yield): mp 134-135 °C; ^{1}H NMR [$(CD_3)_2SO$] δ 8.04 (s, 1 H), 7.98 (br d, *J* = 1.1 Hz, 1 H), 7.79 (br dd, *J* = 8.0, 1.2 Hz, 1 H), 7.63 (d, *J* = 8.0 Hz, 1 H), 7.46 (br d, *J* = 8.7 Hz, 2 H), 7.44 (br d, *J* = 8.7 Hz, 2 H), 4.78-4.68 (m, 3 H), 4.50 (br d, *J* = 11.9 Hz, 1 H), 4.35-4.22 (m, 3 H); ^{13}C NMR [$(CD_3)_2SO$] δ 147.1, 143.6, 142.1, 138.1, 136.7, 132.4, 132.3, 129.5 (q, J_{C-F} = 32.9 Hz), 129.1 (2 C), 127.5 (2 C), 126.6 (q, J_{C-F} = 3.9 Hz), 124.3 (q, J_{C-F} = 3.7 Hz), 123.3 (q, J_{C-F} = 272.4 Hz), 118.0, 69.3, 67.9, 66.6, 46.8. Anal. ($C_{20}H_{15}ClF_3N_3O_4$) C, H, N.

*4.3.2 (6R)-6-{[2'-Chloro-4'-(trifluoromethoxy)[1,1'-biphenyl]-4-yl]methoxy}-2-nitro-6,7-dihydro-5H-imidazo[2,1-b][1,3]oxazine (ent-**30**)*

The title compound was obtained from bromide **29** and [2-chloro-4-(trifluoromethoxy)phenyl]boronic acid (1.8 equiv), using the above procedure at 70 °C for 16 h. Cream solid (63% yield): mp 82-85 °C; ^{1}H NMR [$(CD_3)_2SO$] δ 8.04 (s, 1 H), 7.68 (br d, *J* = 1.8 Hz, 1 H), 7.53 (d, *J* = 8.5 Hz, 1 H), 7.49-7.43 (m, 1 H), 7.42 (s, 4 H), 4.76-4.67 (m, 3 H), 4.50 (br d, *J* = 11.8 Hz, 1 H), 4.35-4.22 (m, 3 H); ^{13}C NMR [$(CD_3)_2SO$] δ 147.7, 147.1, 142.1, 139.0, 137.8, 136.8, 132.8, 132.3, 129.2 (2 C), 127.5 (2 C), 122.6, 120.2, 119.9 (q, J_{C-F} = 257.3 Hz), 118.0, 69.3, 67.9, 66.6, 46.8. Anal. ($C_{20}H_{15}ClF_3N_3O_5$) C, H, N.

*4.3.3 (6S)-6-({5-[2-Chloro-4-(trifluoromethyl)phenyl]pyridin-2-yl}methoxy)-2-nitro-6,7-dihydro-5H-imidazo[2,1-b][1,3]oxazine (**33**)*

The title compound was obtained from (6*S*)-6-[(5-bromopyridin-2-yl)methoxy]-2-nitro-6,7-dihydro-5*H*-imidazo[2,1-*b*][1,3]oxazine [40] (**32**) and [2-chloro-4-(trifluoromethyl)phenyl]boronic acid (1.8 equiv), using the above procedure at 70 °C for 16 h. Pale yellow solid (34% yield): mp 162-164 °C; ^{1}H NMR [$(CD_3)_2SO$] δ 8.63 (br d, *J* = 2.3 Hz,

1 H), 8.05 (s, 1 H), 8.04 (br d, *J* = 1.2 Hz, 1 H), 7.95 (dd, *J* = 8.0, 2.3 Hz, 1 H), 7.84 (br dd, *J* = 8.1, 1.2 Hz, 1 H), 7.71 (d, *J* = 7.9 Hz, 1 H), 7.51 (d, *J* = 8.0 Hz, 1 H), 4.85 (d, *J* = 13.3 Hz, 1 H), 4.80 (d, *J* = 13.3 Hz, 1 H), 4.74 (dt, *J* = 12.0, 2.6 Hz, 1 H), 4.52 (br d, *J* = 11.9 Hz, 1 H), 4.41-4.34 (m, 2 H), 4.28 (dd, *J* = 13.8, 3.5 Hz, 1 H). Anal. ($C_{19}H_{14}ClF_3N_4O_4$) C, H, N.

*4.3.4 (6R)-6-({5-[2-Chloro-4-(trifluoromethyl)phenyl]pyridin-2-yl}methoxy)-2-nitro-6,7-dihydro-5H-imidazo[2,1-b][1,3]oxazine (ent-**33**)*

The title compound was obtained from bromide *ent*-**32** and [2-chloro-4-(trifluoromethyl)phenyl]boronic acid (1.8 equiv), using the above procedure at 70 °C for 16 h. Pale yellow solid (41% yield): mp 160-161 °C; ^{1}H NMR [$(CD_3)_2SO$] δ 8.63 (br d, *J* = 2.2 Hz, 1 H), 8.05 (s, 1 H), 8.04 (br d, *J* = 1.2 Hz, 1 H), 7.95 (dd, *J* = 8.1, 2.3 Hz, 1 H), 7.84 (br dd, *J* = 8.1, 1.2 Hz, 1 H), 7.71 (d, *J* = 7.9 Hz, 1 H), 7.51 (d, *J* = 8.2 Hz, 1 H), 4.85 (d, *J* = 13.3 Hz, 1 H), 4.80 (d, *J* = 13.3 Hz, 1 H), 4.74 (dt, *J* = 12.0, 2.6 Hz, 1 H), 4.52 (br d, *J* = 11.9 Hz, 1 H), 4.41-4.34 (m, 2 H), 4.27 (dd, *J* = 13.8, 3.5 Hz, 1 H); ^{13}C NMR [$(CD_3)_2SO$] δ 157.7, 148.6, 147.1, 142.1, 140.6, 137.6, 132.7, 132.6, 132.1, 130.2 (q, J_{C-F} = 32.8 Hz), 126.7 (q, J_{C-F} = 3.6 Hz), 124.5 (q, J_{C-F} = 3.8 Hz), 123.3 (q, J_{C-F} = 273.2 Hz), 120.9, 118.0, 70.6, 68.0, 67.2, 46.7. Anal. ($C_{19}H_{14}ClF_3N_4O_4$) C, H, N.

*4.4 General procedure for the syntheses of ent-**19** and ent-**20***

A mixture of bromide **37** (300 mg, 1.0 equiv), arylboronic acid (1.8 equiv) and [1,1′-bis(diphenylphosphino)ferrocene]dichloropalladium(II) (0.11 equiv) in DMF (6 mL), toluene (3.5 mL), and EtOH (2.5 mL) was degassed for 10 min (vacuum pump) and then N_2 was added. An aqueous solution of sodium carbonate (1.6 mL of 2 M, 3.2 mmol) was added by syringe, the stirred mixture was again degassed for 10 min, and then N_2 was added. The resulting mixture was stirred at 89 °C for 62 min and then cooled, diluted with aqueous $NaHCO_3$ (50 mL), and extracted with CH_2Cl_2 (5 x 50 mL). The combined extracts were evaporated to dryness under reduced pressure (at 30 °C) and the residue was chromatographed on silica gel (0-0.75% MeOH/CH_2Cl_2) and then crystallized to afford the required products.

*4.4.1 (6R)-2-Nitro-6-[(3-{5-[4-(trifluoromethyl)phenyl]pyridin-2-yl}prop-2-yn-1-yl)oxy]-6,7-dihydro-5H-imidazo[2,1-b][1,3]oxazine (ent-**19**)*

The title compound was obtained from bromide **37** and [4-(trifluoromethyl)phenyl]boronic acid. Pale yellow-brown solid (60% yield): mp (MeOH/CH_2Cl_2/hexane) 218-221 °C; ^{1}H NMR [$(CD_3)_2SO$] δ 8.98 (br d, *J* = 2.4 Hz, 1 H), 8.21 (dd, *J* = 8.2, 2.4 Hz, 1 H), 8.06 (s, 1 H), 8.01 (br d, *J* = 8.2 Hz, 2 H), 7.87 (br d, *J* = 8.3 Hz, 2 H), 7.70 (br d, *J* = 8.2 Hz, 1 H), 4.69 (dt, *J* = 12.1, 3.2 Hz, 1 H), 4.66 (s, 2 H), 4.51 (br d, *J* = 12.1 Hz, 1 H), 4.44-4.39 (m, 1 H), 4.33 (dt, *J* = 13.7, 2.1 Hz, 1 H), 4.27 (dd, *J* = 13.6, 3.2 Hz, 1 H); ^{13}C NMR [$(CD_3)_2SO$] δ 148.4, 147.0, 142.1, 141.4, 140.3, 135.0, 133.6, 128.8 (q, J_{C-F} = 31.8 Hz), 127.8 (2 C), 127.3, 126.0 (q, J_{C-F} = 3.7 Hz, 2 C), 124.2 (q, J_{C-F} = 272.1 Hz), 118.0, 86.0, 85.6, 67.8, 66.4, 56.1, 46.6; HRESIMS calcd for $C_{21}H_{16}F_3N_4O_4$ *m/z* $[M + H]^+$ 445.1118, found 445.1136; HPLC purity: 99.8%.

*4.4.2 (6R)-2-Nitro-6-[(3-{5-[4-(trifluoromethoxy)phenyl]pyridin-2-yl}prop-2-yn-1-yl)oxy]-6,7-dihydro-5H-imidazo[2,1-b][1,3]oxazine (ent-**20**)*

The title compound was obtained from bromide **37** and [4-(trifluoromethoxy)phenyl]boronic acid. Light yellow-orange solid (63% yield): mp (MeOH/CH_2Cl_2/hexane) 205-208 °C; ^{1}H NMR [$(CD_3)_2SO$] δ 8.93 (br d, *J* = 2.4 Hz, 1 H), 8.15 (dd, *J* = 8.2, 2.4 Hz, 1 H), 8.05 (s, 1 H), 7.91 (br d, *J* = 8.9 Hz, 2 H), 7.67 (br d, *J* = 8.2 Hz, 1 H), 7.51 (br d, *J* = 8.0 Hz, 2 H), 4.69 (dt, *J* = 12.1, 2.5 Hz, 1 H), 4.65 (s, 2 H), 4.51 (br d, *J* = 11.9 Hz, 1 H), 4.43-4.39 (m, 1 H), 4.33 (dt, *J* = 13.7, 1.9 Hz, 1 H), 4.27 (dd, *J* = 13.6, 3.2 Hz, 1 H); ^{13}C NMR [$(CD_3)_2SO$] δ 148.6, 148.2, 147.0, 142.1, 140.8, 135.5, 134.7, 133.8, 129.0 (2 C), 127.2, 121.7 (2 C), 120.1 (q, J_{C-F} = 256.5

Hz), 118.0, 85.7, 67.8, 66.3, 56.1, 54.9, 46.6; HRESIMS calcd for $C_{21}H_{16}F_3N_4O_5$ *m/z* $[M + H]^+$ 461.1067, found 461.1086; HPLC purity: 99.9%.

*4.5 General procedure for the syntheses of intermediate alcohols **39-41***

A mixture of 2-chloro-1-[2-(2-methyloxiran-2-yl)ethyl]-4-nitro-1*H*-imidazole [31] (**38**) (250 mg, 1.0 equiv), powdered potassium carbonate (2.0 equiv) and the appropriately substituted phenol (2.0 equiv) in anhydrous 2-butanone (2.5 mL) was stirred in a sealed vial at 82 °C for 24 h. The resulting cooled mixture was added to water (50 mL), treated with aqueous citric acid (2.2 mL of a 1 M solution), and extracted with CH_2Cl_2 (6 x 50 mL). The combined extracts were evaporated to dryness under reduced pressure (at 30 °C) and the residue was chromatographed on silica gel (0-2% EtOAc/CH_2Cl_2) to afford the required products.

*4.5.1 4-(2-Chloro-4-nitro-1H-imidazol-1-yl)-1-[2-chloro-4-(trifluoromethoxy)phenoxy]-2-methylbutan-2-ol (**39**)*
The title compound was obtained from epoxide **38** and 2-chloro-4-(trifluoromethoxy)phenol. Cream solid (72% yield): mp (pentane triturate) 92-93 °C; ^{1}H NMR ($CDCl_3$) δ 7.82 (s, 1 H), 7.32 (br d, *J* = 2.3 Hz, 1 H), 7.13 (br dd, *J* = 9.0, 2.0 Hz, 1 H), 6.90 (d, *J* = 9.0 Hz, 1 H), 4.38-4.22 (m, 2 H), 3.91 (d, *J* = 8.9 Hz, 1 H), 3.88 (d, *J* = 8.9 Hz, 1 H), 2.37 (br s, 1 H), 2.29 (ddd, *J* = 13.9, 9.9, 6.1 Hz, 1 H), 2.07 (ddd, *J* = 13.8, 9.8, 6.2 Hz, 1 H), 1.44 (s, 3 H). Anal. ($C_{15}H_{14}Cl_2F_3N_3O_5$) C, H, N.

*4.5.2 4-(2-Chloro-4-nitro-1H-imidazol-1-yl)-1-[3-chloro-4-(trifluoromethoxy)phenoxy]-2-methylbutan-2-ol (**40**)*
The title compound was obtained from epoxide **38** and 3-chloro-4-(trifluoromethoxy)phenol, using the above procedure for 17 h. Pale yellow oil (68% yield); ^{1}H NMR ($CDCl_3$) δ 7.82 (s, 1 H), 7.26 (br d, *J* = 9.0 Hz, 1 H), 7.03 (d, *J* = 3.0 Hz, 1 H), 6.83 (dd, *J* = 9.1, 3.0 Hz, 1 H), 4.34-4.20 (m, 2 H), 3.85 (d, *J* = 8.9 Hz, 1 H), 3.82 (d, *J* = 8.9 Hz, 1 H), 2.22 (ddd, *J* = 13.8, 9.4, 6.5 Hz, 1 H), 2.18 (br s, 1 H), 2.03 (ddd, *J* = 13.7, 9.7, 6.5 Hz, 1 H), 1.41 (s, 3 H); HRESIMS calcd for $C_{15}H_{15}Cl_2F_3N_3O_5$ *m/z* $[M + H]^+$ 446.0309, 444.0335, found 446.0306, 444.0337.

*4.5.3 4-(2-Chloro-4-nitro-1H-imidazol-1-yl)-1-[3-fluoro-4-(trifluoromethoxy)phenoxy]-2-methylbutan-2-ol (**41**)*
The title compound was obtained from epoxide **38** and 3-fluoro-4-(trifluoromethoxy)phenol (2.1 equiv), using the above procedure for 17 h. Pale yellow oil (68% yield); ^{1}H NMR ($CDCl_3$) δ 7.82 (s, 1 H), 7.24 (br t, *J* = 8.8 Hz, 1 H), 6.77 (dd, *J* = 11.3, 2.9 Hz, 1 H), 6.69 (ddd, *J* = 9.1, 2.9, 1.6 Hz, 1 H), 4.34-4.20 (m, 2 H), 3.84 (d, *J* = 8.9 Hz, 1 H), 3.81 (d, *J* = 8.9 Hz, 1 H), 2.22 (ddd, *J* = 13.8, 9.3, 6.5 Hz, 1 H), 2.19 (br s, 1 H), 2.04 (ddd, *J* = 13.9, 9.5, 6.7 Hz, 1 H), 1.41 (s, 3 H); HRESIMS calcd for $C_{15}H_{15}ClF_4N_3O_5$ *m/z* $[M + H]^+$ 430.0607, 428.0631, found 430.0611, 428.0629.

*4.6 General procedure for the syntheses of **42-44***

Sodium hydride (60% in mineral oil, unwashed, 1.5 equiv) was added to a solution of the alcohol (**39**, **40**, or **41**, 1.0 equiv) in anhydrous DMF (2 mL/100 mg of alcohol) under N_2. The mixture was immediately degassed and resealed under N_2 and then stirred at 20 °C for 160 min. The resulting mixture was rapidly cooled (CO_2/acetone), quenched with ice/aqueous $NaHCO_3$ (10 mL), added to brine (40 mL), and extracted with CH_2Cl_2 (7 x 50 mL). The combined extracts were evaporated to dryness under reduced pressure (at 30 °C) and the residue was chromatographed on silica gel (CH_2Cl_2) and then crystallized to afford the required products.

*4.6.1 7-{[2-Chloro-4-(trifluoromethoxy)phenoxy]methyl}-7-methyl-2-nitro-6,7-dihydro-5H-imidazo[2,1-b][1,3]oxazine (**42**)*

The title compound was obtained from alcohol **39**. Cream solid (77% yield): mp (CH_2Cl_2/pentane) 120-121 °C; ^{1}H NMR [$(CD_3)_2SO$] δ 8.11 (s, 1 H), 7.58 (br d, *J* = 2.8 Hz, 1 H), 7.38 (br dd, *J* = 9.1, 2.8 Hz, 1 H), 7.30 (d, *J* = 9.2 Hz, 1 H), 4.34 (d, *J* = 10.8 Hz, 1 H), 4.31 (d, *J* = 10.9 Hz, 1 H), 4.24 (ddd, *J* = 12.9, 6.9, 6.0 Hz, 1 H), 4.15 (ddd, *J* = 13.0, 7.1, 5.9 Hz, 1 H), 2.42 (ddd, *J* = 14.4, 7.1, 6.0 Hz, 1 H), 2.23 (ddd, *J* = 14.3, 6.9, 6.0 Hz, 1 H), 1.52 (s, 3 H); ^{13}C NMR [$(CD_3)_2SO$] δ 152.7, 147.3, 142.1, 141.6 (q, J_{C-F} = 1.9 Hz), 123.3. 121.9, 121.4, 120.0 (q, J_{C-F} = 256.2 Hz), 117.8, 114.6, 80.2, 73.5, 39.7, 27.3, 21.8. Anal. ($C_{15}H_{13}ClF_3N_3O_5$) C, H, N.

*4.6.2 7-{[3-Chloro-4-(trifluoromethoxy)phenoxy]methyl}-7-methyl-2-nitro-6,7-dihydro-5H-imidazo[2,1-b][1,3]oxazine (**43**)*

The title compound was obtained from alcohol **40**, using the above procedure for 3 h. Cream solid (57% yield): mp (CH_2Cl_2/pentane) 83-85 °C; ^{1}H NMR [$(CD_3)_2SO$] δ 8.10 (s, 1 H), 7.50 (br d, *J* = 9.1 Hz, 1 H), 7.34 (d, *J* = 2.9 Hz, 1 H), 7.06 (dd, *J* = 9.1, 3.0 Hz, 1 H), 4.25 (s, 2 H), 4.19 (dt, *J* = 13.1, 6.2 Hz, 1 H), 4.13 (ddd, *J* = 13.2, 7.8, 5.8 Hz, 1 H), 2.37 (ddd, *J* = 14.1, 7.7, 6.3 Hz, 1 H), 2.17 (dt, *J* = 14.3, 5.9 Hz, 1 H), 1.49 (s, 3 H); ^{13}C NMR [$(CD_3)_2SO$] δ 157.4, 147.2, 142.2, 137.9 (q, J_{C-F} = 1.9 Hz), 127.0, 124.2, 120.1 (q, J_{C-F} = 257.5 Hz), 117.8, 116.5, 115.3, 80.4, 72.5, 39.5, 26.9, 21.3. Anal. ($C_{15}H_{13}ClF_3N_3O_5$) C, H, N.

*4.6.3 7-{[3-Fluoro-4-(trifluoromethoxy)phenoxy]methyl}-7-methyl-2-nitro-6,7-dihydro-5H-imidazo[2,1-b][1,3]oxazine (**44**)*

The title compound was obtained from alcohol **41**, using the above procedure for 2.5 h. Cream solid (65% yield): mp (CH_2Cl_2/pentane) 144-146 °C; ^{1}H NMR [$(CD_3)_2SO$] δ 8.10 (s, 1 H), 7.49 (br t, *J* = 9.1 Hz, 1 H), 7.21 (dd, *J* = 12.4, 2.9 Hz, 1 H), 6.91 (ddd, *J* = 9.2, 2.9, 1.5 Hz, 1 H), 4.25 (d, *J* = 10.7 Hz, 1 H), 4.22 (d, *J* = 10.8 Hz, 1 H), 4.19 (dt, *J* = 13.1, 6.1 Hz, 1 H), 4.13 (ddd, *J* = 13.2, 8.1, 5.7 Hz, 1 H), 2.37 (ddd, *J* = 14.3, 8.0, 6.3 Hz, 1 H), 2.18 (dt, *J* = 14.4, 5.8 Hz, 1 H), 1.49 (s, 3 H); ^{13}C NMR [$(CD_3)_2SO$] δ 158.1 (d, J_{C-F} = 9.8 Hz), 154.2 (d, J_{C-F} = 249.3 Hz), 147.1, 142.2, 128.9 (d, J_{C-F} = 10.8 Hz), 124.8, 120.1 (q, J_{C-F} = 257.2 Hz), 117.8, 111.6 (d, J_{C-F} = 3.0 Hz), 104.1 (d, J_{C-F} = 22.1 Hz), 80.3, 72.6, 39.5, 26.9, 21.2. Anal. ($C_{15}H_{13}F_4N_3O_5$) C, H, N. HPLC purity: 96.6%.

*4.7 Syntheses of thiazine derivatives **46-48***

*4.7.1 2-Chloro-1-[2-(2-methylthiiran-2-yl)ethyl]-4-nitro-1H-imidazole (**45**)*

A solution of epoxide **38** (166 mg, 0.717 mmol) in CH_2Cl_2 (6.5 mL) was treated with thiourea on silica gel [42] (1.40 g, containing 0.931 mmol of thiourea). The mixture was stirred at 20 °C for 6.5 h and then filtered, washing with CH_2Cl_2. The filtrate was concentrated under reduced pressure (at 25 °C) to give an oil, which was chromatographed on silica gel (3:1 CH_2Cl_2/petroleum ether then CH_2Cl_2) to afford the title compound. Pale brown solid (140 mg, 79% yield): mp (CH_2Cl_2/pentane) 70-71 °C; ^{1}H NMR ($CDCl_3$) δ 7.76 (s, 1 H), 4.27 (ddd, *J* = 14.1, 9.7, 5.8 Hz, 1 H), 4.17 (ddd, *J* = 14.1, 9.3, 6.0 Hz, 1 H), 2.55 (ddd, *J* = 13.9, 9.3, 5.8 Hz, 1 H), 2.45 (d, *J* = 1.4 Hz, 1 H), 2.38 (d, *J* = 1.2 Hz, 1 H), 1.89 (ddd, *J* = 13.9, 9.7, 6.1 Hz, 1 H), 1.65 (s, 3 H). Anal. ($C_8H_{10}ClN_3O_2S$) C, H, N.

*4.7.2 7-Methyl-2-nitro-7-{[4-(trifluoromethoxy)phenoxy]methyl}-6,7-dihydro-5H-imidazo[2,1-b][1,3]thiazine (**46**)*

A mixture of thiirane **45** (159 mg, 0.642 mmol), powdered potassium carbonate (887 mg, 6.42 mmol) and 4-(trifluoromethoxy)phenol (0.85 mL, 6.56 mmol) in anhydrous 2-butanone (1.6 mL) was stirred in a sealed vial at 80 °C for 10.5 h. The resulting cooled mixture was added to

water (50 mL) and extracted with CH_2Cl_2 (6 x 50 mL). The combined extracts were evaporated to dryness under reduced pressure (at 30 °C) and the residue was chromatographed twice on silica gel (firstly with 0-25% EtOAc/petroleum ether and secondly with CH_2Cl_2) to afford the title compound. Pale yellow solid (68 mg, 27% yield): mp (CH_2Cl_2/pentane) 130-132 °C; ^{1}H NMR [$(CD_3)_2SO$] δ 8.46 (s, 1 H), 7.30 (br d, *J* = 9.0 Hz, 2 H), 7.06 (br d, *J* = 9.2 Hz, 2 H), 4.32-4.18 (m, 3 H), 4.17 (d, *J* = 9.8 Hz, 1 H), 2.43 (ddd, *J* = 14.6, 6.4, 4.7 Hz, 1 H), 2.25 (ddd, *J* = 14.5, 8.4, 5.2 Hz, 1 H), 1.58 (s, 3 H); ^{13}C NMR [$(CD_3)_2SO$] δ 157.0, 146.2, 142.2 (q, J_{C-F} = 1.6 Hz), 139.0, 123.0, 122.5 (2 C), 120.1 (q, J_{C-F} = 255.3 Hz), 116.1 (2 C), 74.1, 47.3, 42.3, 31.9, 24.8. Anal. ($C_{15}H_{14}F_3N_3O_4S$) C, H, N.

*4.7.3 7-Methyl-2-nitro-7-{[4-(trifluoromethoxy)phenoxy]methyl}-6,7-dihydro-5H-imidazo[2,1-b][1,3]thiazine 8-oxide (**47**)*

A mixture of thiazine **46** (69.4 mg, 0.178 mmol), powdered disodium hydrogen phosphate (56.1 mg, 0.395 mmol), and *m*-CPBA (47.2 mg of 70%, 0.191 mmol) in CH_2Cl_2 (5 mL) was stirred at 20 °C for 17 h. The resulting mixture was added to an ice-cold aqueous solution of sodium sulphite (50 mL of 10%) and extracted with CH_2Cl_2 (4 x 50 mL). The extracts were sequentially washed with cold aqueous $NaHCO_3$ (50 mL) and then concentrated under reduced pressure, and the remaining oil was chromatographed on silica gel (0-0.5% MeOH/CH_2Cl_2) to afford the title compound as a 1:1 mixture of diastereomers. White solid (69.5 mg, 96% yield): mp (Et_2O/pentane) 159-161 °C; ^{1}H NMR ($CDCl_3$) δ 7.91, 7.90 (2 s, 1 H), 7.18, 7.13 (2 br d, *J* = 9.0 Hz, 2 H), 6.98, 6.68 (2 br d, *J* = 9.2 Hz, 2 H), 4.48 (ddd, *J* = 13.8, 5.8, 2.1 Hz, 0.5 H), 4.41 (ddd, *J* = 13.6, 5.5, 4.5 Hz, 0.5 H), 4.37-4.23 (m, 3 x 0.5 H), 4.17 (s, 2 x 0.5 H), 4.01 (d, *J* = 9.4 Hz, 0.5 H), 3.04 (ddd, *J* = 15.1, 12.8, 5.8 Hz, 0.5 H), 2.92 (ddd, *J* = 15.6, 10.5, 5.6 Hz, 0.5 H), 2.36 (dt, *J* = 15.6, 4.5 Hz, 0.5 H), 2.05 (ddd, *J* = 15.2, 4.5, 2.1 Hz, 0.5 H), 1.61, 1.44 (2 s, 3 H). Anal. ($C_{15}H_{14}F_3N_3O_5S$) C, H, N.

*4.7.4 7-Methyl-2-nitro-7-{[4-(trifluoromethoxy)phenoxy]methyl}-6,7-dihydro-5H-imidazo[2,1-b][1,3]thiazine 8,8-dioxide (**48**)*

A mixture of thiazine **46** (20.0 mg, 0.051 mmol), powdered disodium hydrogen phosphate (25.6 mg, 0.180 mmol), and *m*-CPBA (27.5 mg of 70%, 0.112 mmol) in CH_2Cl_2 (2 mL) was stirred at 20 °C for 24 h. Additional *m*-CPBA (9.5 mg of 70%, 0.039 mmol) was added and the mixture was stirred at 20 °C for a further 29 h. The resulting mixture was added to an ice-cold aqueous solution of sodium sulphite (50 mL of 2.5%) and extracted with CH_2Cl_2 (4 x 50 mL). The extracts were sequentially washed with cold aqueous $NaHCO_3$ (50 mL) and then concentrated under reduced pressure, and the remaining oil was chromatographed on silica gel (CH_2Cl_2) to afford the title compound. White solid (19 mg, 88% yield): mp (CH_2Cl_2/pentane) 143-145 °C; ^{1}H NMR [$(CD_3)_2SO$] δ 8.69 (s, 1 H), 7.31 (br d, *J* = 8.5 Hz, 2 H), 6.96 (br d, *J* = 9.2 Hz, 2 H), 4.47 (d, *J* = 10.4 Hz, 1 H), 4.45-4.31 (m, 3 H), 2.71 (dt, *J* = 15.7, 5.6 Hz, 1 H), 2.62 (ddd, *J* = 15.8, 7.2, 5.9 Hz, 1 H), 1.58 (s, 3 H); ^{13}C NMR [$(CD_3)_2SO$] δ 156.3, 145.9, 142.4 (q, J_{C-F} = 1.5 Hz), 141.4, 123.2, 122.6 (2 C), 120.1 (q, J_{C-F} = 255.4 Hz), 116.0 (2 C), 69.4, 61.4, 43.2, 30.2, 14.8. Anal. ($C_{15}H_{14}F_3N_3O_6S$) C, H, N.

*4.8 Synthesis of triazole **56***

*4.8.1 4-(Benzyloxy)-2-methyl-1-[4-(trifluoromethoxy)phenoxy]butan-2-ol (**50**)*

The title compound was obtained from 2-[2-(benzyloxy)ethyl]-2-methyloxirane [43] (**49**), potassium carbonate (1.5 equiv) and 4-(trifluoromethoxy)phenol (1.6 equiv), using the general procedure described in section 4.5 above for 4.5 days, and following chromatography on silica gel (0-3% then 25% Et_2O/petroleum ether). Pale yellow oil (81% yield); ^{1}H NMR ($CDCl_3$) δ 7.37-7.26 (m, 5 H), 7.12 (br d, *J* = 9.1 Hz, 2 H), 6.85 (br d, *J* = 9.2 Hz, 2 H), 4.54 (d, *J* = 11.8

Hz, 1 H), 4.50 (d, *J* = 11.8 Hz, 1 H), 3.81 (d, *J* = 8.9 Hz, 1 H), 3.78 (d, *J* = 8.8 Hz, 1 H), 3.78-3.68 (m, 2 H), 3.54 (s, 1 H), 2.02 (ddd, *J* = 14.7, 6.2, 4.8 Hz, 1 H), 1.94 (ddd, *J* = 14.8, 7.1, 5.1 Hz, 1 H), 1.33 (s, 3 H); HRESIMS calcd for $C_{19}H_{21}F_3NaO_4$ *m/z* $[M + Na]^+$ 393.1284, found 393.1276.

*4.8.2 ({4-(Benzyloxy)-2-methyl-1-[4-(trifluoromethoxy)phenoxy]butan-2-yl}oxy)(tert-butyl)dimethylsilane (**51**)*

tert-Butyldimethylsilyl trifluoromethanesulfonate (1.35 mL, 7.71 mmol) was added dropwise to a stirred mixture of alcohol **50** (1.59 g, 4.29 mmol) and 2,6-dimethylpyridine (1.05 mL, 9.02 mmol) in anhydrous CH_2Cl_2 (24 mL) under N_2 at 0 °C. The mixture was stirred at 0 °C for 30 min and at 20 °C for 65 h, and then added to ice/ aqueous $NaHCO_3$ (50 mL) and extracted with CH_2Cl_2 (5 x 50 mL). The combined extracts were evaporated to dryness under reduced pressure (at 30 °C) and the residue was chromatographed on silica gel (0-2% Et_2O/petroleum ether) to afford the title compound. Colourless oil (1.98 g, 95% yield); ^{1}H NMR ($CDCl_3$) δ 7.35-7.23 (m, 5 H), 7.12 (br d, *J* = 9.1 Hz, 2 H), 6.84 (br d, *J* = 9.2 Hz, 2 H), 4.49 (d, *J* = 12.0 Hz, 1 H), 4.46 (d, *J* = 12.0 Hz, 1 H), 3.76 (d, *J* = 8.9 Hz, 1 H), 3.74 (d, *J* = 9.0 Hz, 1 H), 3.72-3.60 (m, 2 H), 2.00 (dt, *J* = 14.0, 7.0 Hz, 1 H), 1.90 (ddd, *J* = 14.0, 7.0, 6.3 Hz, 1 H), 1.35 (s, 3 H), 0.83 (s, 9 H), 0.09 (s, 3 H), 0.06 (s, 3 H); HRESIMS calcd for $C_{25}H_{35}F_3NaO_4Si$ *m/z* $[M + Na]^+$ 507.2149, found 507.2137.

*4.8.3 3-[(tert-Butyldimethylsilyl)oxy]-3-methyl-4-[4-(trifluoromethoxy)phenoxy]butan-1-ol (**52**)*

A mixture of benzyl ether **51** (1.98 g, 4.09 mmol) and 10% Pd-C (200 mg) in 50% EtOH/EtOAc (60 mL) was hydrogenated at 60 psi for 42 h, and then the catalyst was removed by filtration through Celite, washing with 33% MeOH/CH_2Cl_2. The filtrate was concentrated under reduced pressure (at 30 °C), and the residual oil was chromatographed on silica gel (0-2% then 20% Et_2O/petroleum ether) to afford the title compound. Colourless oil (1.61 g, 100% yield); ^{1}H NMR ($CDCl_3$) δ 7.15 (br d, *J* = 9.1 Hz, 2 H), 6.88 (br d, *J* = 9.2 Hz, 2 H), 3.91-3.79 (m, 3 H), 3.78 (d, *J* = 8.8 Hz, 1 H), 2.29 (t, *J* = 5.3 Hz, 1 H), 1.98 (ddd, *J* = 14.3, 6.6, 5.6 Hz, 1 H), 1.84 (ddd, *J* = 14.3, 6.7, 5.6 Hz, 1 H), 1.41 (s, 3 H), 0.88 (s, 9 H), 0.16 (s, 3 H), 0.12 (s, 3 H); HRESIMS calcd for $C_{18}H_{29}F_3NaO_4Si$ *m/z* $[M + Na]^+$ 417.1679, found 417.1671.

*4.8.4 tert-Butyl({4-iodo-2-methyl-1-[4-(trifluoromethoxy)phenoxy]butan-2-yl}oxy)dimethylsilane (**53**)*

A solution of iodine (1.47 g, 5.79 mmol) in anhydrous CH_2Cl_2 (7 x 6 mL) was added in portions over 40 min (with water bath cooling) to a mixture of alcohol **52** (1.61 g, 4.08 mmol), imidazole (724 mg, 10.6 mmol) and triphenylphosphine (1.40 g, 5.34 mmol) in anhydrous CH_2Cl_2 (24 mL) under N_2. After being stirred at 20 °C for 39 h, the mixture was concentrated under reduced pressure (at 25 °C), and then dissolved in CH_2Cl_2 (5 mL) and added to excess petroleum ether (200 mL) at the top of a silica gel column (40 g in petroleum ether), rinsing residues onto the column with minimal additional CH_2Cl_2 (5 x 3 mL). Elution of this mixture and then 5% Et_2O/petroleum ether gave the title compound. Colourless oil (1.98 g, 96% yield); ^{1}H NMR ($CDCl_3$) δ 7.15 (br d, *J* = 9.1 Hz, 2 H), 6.87 (br d, *J* = 9.1 Hz, 2 H), 3.74 (d, *J* = 8.8 Hz, 1 H), 3.67 (d, *J* = 8.8 Hz, 1 H), 3.27 (ddd, *J* = 11.9, 9.1, 5.2 Hz, 1 H), 3.22 (ddd, *J* = 11.8, 9.1, 5.4 Hz, 1 H), 2.36 (ddd, *J* = 13.7, 12.1, 5.4 Hz, 1 H), 2.20 (ddd, *J* = 13.7, 12.0, 5.2 Hz, 1 H), 1.33 (s, 3 H), 0.87 (s, 9 H), 0.12 (s, 3 H), 0.09 (s, 3 H); HRESIMS calcd for $C_{18}H_{28}F_3INaO_3Si$ *m/z* $[M + Na]^+$ 527.0697, found 527.0688.

*4.8.5 5-Methyl-2-nitro-5-{[4-(trifluoromethoxy)phenoxy]methyl}-6,7-dihydro-5H-[1,2,4]triazolo[5,1-b][1,3]oxazine (**56**)*

A mixture of iodide **53** (1.98 g, 3.93 mmol), 5-bromo-3-nitro-1*H*-1,2,4-triazole (**54**) (872 mg, 4.52 mmol) and powdered potassium carbonate (629 mg, 4.55 mmol) in anhydrous DMF (8 mL) under N_2 was stirred at 73 °C for 61 h. The cooled mixture was evaporated to dryness under reduced pressure (at 25 °C), and the residue was chromatographed on silica gel (20-40% CH_2Cl_2/petroleum ether) to afford the crude adduct **55** (0.995 g, 45% yield) as a red-brown oil. This oil was immediately dissolved in anhydrous distilled THF (20 mL), and the resulting solution was sealed under N_2, cooled to 0 °C, and treated with TBAF (10.5 mL of a 1 M solution in THF, 10.5 mmol). The mixture was stirred at 0-20 °C for 24 h, and then added to ice/aqueous $NaHCO_3$ (100 mL) and extracted with EtOAc (4 x 100 mL). The combined extracts were evaporated to dryness under reduced pressure (at 30 °C), and the residue was chromatographed three times on silica gel (firstly with 0-33% EtOAc/petroleum ether, secondly with 75-90% CH_2Cl_2/petroleum ether, and thirdly with 50-60% Et_2O/petroleum ether and then Et_2O) to afford the title compound. Pale yellow gum (185 mg, 28% yield); ^{1}H NMR [$(CD_3)_2SO$] δ 7.31 (br d, *J* = 9.1 Hz, 2 H), 7.07 (br d, *J* = 9.2 Hz, 2 H), 4.36 (dt, *J* = 13.0, 6.1 Hz, 1 H), 4.32 (ddd, *J* = 13.1, 7.4, 5.7 Hz, 1 H), 4.29 (s, 2 H), 2.54 (dt, *J* = 14.5, 7.3 Hz, 1 H), 2.36 (dt, *J* = 14.6, 5.9 Hz, 1 H), 1.56 (s, 3 H); ^{13}C NMR [$(CD_3)_2SO$] δ 158.2, 156.8, 155.6, 142.2 (q, $J_{C\text{-}F}$ = 2.0 Hz), 122.6 (2 C), 120.1 (q, $J_{C\text{-}F}$ = 255.4 Hz), 116.0 (2 C), 82.9, 72.1, 41.7, 27.1, 21.1. Anal. ($C_{14}H_{13}F_3N_4O_5$) C, H, N. HPLC purity: 100%.

4.9 Biological and physicochemical assays

4.9.1 In vitro parasite growth inhibition and cytotoxicity assays

An initial evaluation of 58 pretomanid analogues (including **23**, **25** and *ent*-**25**) against *T. cruzi* intracellular amastigotes at the Swiss Tropical institute was conducted according to a standard method [10], which employs a Tulahuen C2C4 strain of *T. cruzi* that expresses the β-galactosidase gene (*LacZ*) and L6 rat skeletal myoblast cells as the host cells. The subsequent screening of ~900 library compounds against Y strain *T. cruzi* amastigotes in U2OS cells was performed at the Institut Pasteur Korea, South Korea, using a seven-point 3-fold dilution image-based assay (with 10 μg/mL being the highest test concentration) to generate % inhibition data, as reported [8]. Follow-up IC_{50}/IC_{90} testing against Tulahuen strain TcVI *T. cruzi* (expressing the β-galactosidase gene) in L6 cells and assessment of cytotoxicity toward L6 host cells was carried out at Murdoch University, Australia, according to the published protocols [32]. Selected leads were further profiled for potency and maximum activity against Tulahuen strain *T. cruzi* amastigotes in 3T3 fibroblasts (host cells) by employing a 48-hour high content image-based assay conducted at Discovery Biology, Griffith Institute for Drug Discovery, Griffith University, Australia, as described in a recent article [47].

4.9.2 T. cruzi CYP51 inhibition assay

Selected leads were screened against Tulahuen strain *T. cruzi* CYP51 (sterol 14α-demethylase) in a high throughput fluorescence-based assay run at the Drug Discovery Unit, University of Dundee, United Kingdom, according to the published method [46].

4.9.3 CYP3A4 inhibition assay

Five hit compounds (**13**-**17**) were assessed for their ability to inhibit CYP3A4/5-mediated 6β-hydroxylation of testosterone (50 μM) in human liver microsomes at the Centre for Drug Candidate Optimisation, Monash University, Australia, using a standard protocol [32].

4.9.4 Microsomal stability assays

Microsomal stability studies on compounds *ent*-**16**, *ent*-**19**, *ent*-**20**, *ent*-**30**, **42**-**44**, **48**, **56**, **65**, and **70** were performed by WuXi AppTec (Shanghai) Co., Ltd., Shanghai, China, using a reported method [30] (except that the concentration of microsomal protein was 0.4 mg/mL).

Five hits (**13-17**) were evaluated for stability toward human liver microsomes at the Centre for Drug Candidate Optimisation, Monash University, Australia, via a similar procedure [32].

4.9.5 hERG assay

The effects of compounds *rac*-**11**, **16** and **17** on cloned hERG potassium channels expressed in Chinese hamster ovary cells were assessed by WuXi AppTec (Shanghai) Co., Ltd., using the automated patch clamp method. Six concentrations (0.12, 0.37, 1.11, 3.33, 10, and 30 μM) were tested (at room temperature), and at least two replicates were obtained for each.

4.9.6 Solubility measurements

The solid compound sample was mixed with water or 0.1 M HCl (enough to make a 2 mM solution) in an Eppendorf tube, and the suspension was sonicated for 15 min and then centrifuged at 13000 rpm for 6 min. An aliquot of the clear supernatant was diluted 2-fold with water (or 0.1 M HCl) and then HPLC was implemented. The kinetic solubility was calculated by comparing the peak area obtained with that from a standard solution of the compound in DMSO (after allowing for varying dilution factors and injection volumes).

4.9.7 Ethics statement for animal experiments

All animal experiments were performed according to institutional ethical guidelines for animal care. Mouse model experiments in London were approved by the LSHTM Ethics Committee and performed under licence PPL70/8207, according to UK Home Office regulations, Animals (Scientific Procedures) Act 1986 and European Directive 2010/63/EU. Pharmacokinetic studies in non-infected mice conformed to the Australian Code of Practice for the Care and Use of Animals for Scientific Purposes and the protocols were approved by the Monash Institute of Pharmaceutical Sciences Animal Ethics Committee. Mouse model experiments in Murdoch were similarly carried out with the approval of the Animal Ethics Committee of Murdoch University.

4.9.8 Mouse pharmacokinetics

The systemic exposures of hit compounds **13-17** were determined at the Centre for Drug Candidate Optimisation, Monash University, Australia, as described [32]. Briefly, the compounds were administered as single oral doses (50 mg/kg) to groups of 3 male Swiss Outbred mice (weighing 25-31 g) using a suspension formulation comprising 7% Tween 80 and 3% EtOH in deionised water. Two blood samples were collected from each mouse to provide duplicate samples (from different mice) at time points of 0.5, 8 and 24 h post-dose. Blood was transferred to heparinised tubes containing a stabilisation cocktail to minimise the potential for degradation, and centrifuged immediately to collect plasma for analysis by LCMS against calibration standards.

4.9.9 Mouse model for acute T. cruzi infection (Murdoch)

Compounds **3** and **17** were tested for *in vivo* efficacy against acute and subchronic phase *T. cruzi* infection at Murdoch University, Australia, according to a reported protocol [32]. Briefly, each test group consisted of 5 female Swiss mice, 8 weeks old, approximately 30 g, infected intraperitoneally with 50,000 bloodform trypomastigotes of *T. cruzi* (Tulahuen strain). Posaconazole (**3**, Noxafil diluted with water for injection; 20 mg/kg) and **17** (in HPMC-SV; 0.5% w/v hydroxypropylmethylcellulose + 0.4% v/v Tween 80 + 0.5% v/v benzyl alcohol in deionised H_2O with 5% v/v DMSO; 50 mg/kg) were dosed orally, once daily for 20 days, commencing on day 8 p.i. Blood parasitemia levels were evaluated over the course of the 20 days of dosing (on days 8 – prior to dosing, 9, 12, 14, 16, 19, 21, and 28 p.i.) by pricking the tail and collecting 3 μL of blood, which was diluted 1:10 with red blood cell lysis and counted under the microscope using a neubauer haemocytometer. At the end of the dosing period and

following 10 days of rest, animals with very low or undetectable parasitemia were immunosuppressed in three cycles, via intraperitoneal administration of cyclophosphamide (50 mg/kg) once daily for 4 days, followed by 3 days of rest (starting on day 37 p.i.). Animals were checked for any recurrence of blood parasitemia periodically during the immunosuppression phase (on days 37 – prior to dosing, 44, 51, and 58 p.i.). If parasite rebound was not observed after three rounds of immunosuppression, the animals were euthanized and tissues (spleen, heart, skeletal muscle and colon) and blood were collected for confirmation of cure by PCR.

4.9.10 Mouse model for chronic T. cruzi infection (London)

Compound **58** was tested for *in vivo* efficacy against chronic *T. cruzi* infection at the London School of Hygiene & Tropical Medicine, United Kingdom, using a published procedure [14]. Briefly, each test group consisted of 5 female BALB/c mice, 8 weeks old, approximately 18 g, infected intraperitoneally with 10^3 bloodstream form trypomastigotes of bioluminescent *T. cruzi* (CL Brener genetically transformed with the construct pTRIX2-RE9h). Reference drugs **1**, **2** and **6** (in HPMC-SV; 0.5% w/v hydroxypropylmethylcellulose + 0.4% v/v Tween 80 + 0.5% v/v benzyl alcohol in deionised H_2O with 5% v/v DMSO; 100 mg/kg) and **58** (in PEG400; 50 mg/kg) were dosed orally, once daily for 5 days, commencing on day 114 p.i., and treated mice were monitored regularly by bioluminescence imaging. All treated mice were then immunosuppressed via intraperitoneal injection of cyclophosphamide (200 mg/kg) given on days 135, 139 and 143 p.i. After final imaging on day 149 p.i., organs were removed and assessed for bioluminescence (days 149-151 p.i.).

Declaration of competing interest

The authors declare no competing financial interests.

Acknowledgments

The authors thank the Drugs for Neglected Diseases *initiative* for financial support through a collaborative research agreement. For this project, DND*i* received financial support from the following donors: Department for International Development (DFID), UK; Federal Ministry of Education and Research (BMBF), through KfW, Germany; Directorate-General for International Cooperation (DGIS), The Netherlands; Ministry of Foreign and European Affairs (MAEE), France; Swiss Agency for Development and Cooperation (SDC), Switzerland; Médecins Sans Frontières (MSF), International. The donors had no role in study design, data collection and analysis, decision to publish, or preparation of the manuscript. The authors also thank Stéphanie Braillard and Fanny Escudié (DND*i*) for coordination support and Sisira Kumara (ACSRC) for the solubility measurements.

Appendix A. Supplementary data

Supplementary data to this article can be found online at https://doi.org/10.1016/j.ejmech.2020.*

References

[1] World Health Organization, Chagas disease (also known as American trypanosomiasis), Available at: https://www.who.int/news-room/fact-sheets/detail/chagas-disease-(american-trypanosomiasis) and https://www.who.int/chagas/epidemiology/en/ (accessed 8 April, 2020).

[2] K.M. Bonney, Chagas disease in the 21st Century: a public health success or an emerging threat?, Parasite 21 (2014) 11, https://doi.org/10.1051/parasite/2014012.

[3] K.C.F. Lidani, F.A. Andrade, L. Bavia, F.S. Damasceno, M.H. Beltrame, I.J. Messias-Reason, T.L. Sandri, Chagas disease: from discovery to a worldwide health problem, Front. Public Health 7 (2019) 166, https://doi.org/10.3389/fpubh.2019.00166.
[4] E. Chatelain, Chagas disease drug discovery: toward a new era, J. Biomol. Screening 20 (2015) 22-35, https://doi.org/10.1177/1087057114550585.
[5] E. Pinheiro, L. Brum-Soares, R. Reis, J.-C. Cubides, Chagas disease: review of needs, neglect, and obstacles to treatment access in Latin America, Rev. Soc. Bras. Med. Trop. 50 (2017) 296-300, https://doi.org/10.1590/0037-8682-0433-2016.
[6] A.F. Francisco, S. Jayawardhana, M.D. Lewis, M.C. Taylor, J.M. Kelly, Biological factors that impinge on Chagas disease drug development, Parasitology 144 (2017) 1871-1880, https://doi.org/10.1017/S0031182017001469.
[7] M. Zrein, E. Chatelain, The unmet medical need for *Trypanosoma cruzi*-infected patients: monitoring the disease status, Biochim. Biophys. Acta Mol. Basis Dis. 1866 (2020) 165628, https://doi.org/10.1016/j.bbadis.2019.165628.
[8] C.B. Moraes, M.A. Giardini, H. Kim, C.H. Franco, A.M. Araujo-Junior, S. Schenkman, E. Chatelain, L.H. Freitas-Junior, Nitroheterocyclic compounds are more efficacious than CYP51 inhibitors against *Trypanosoma cruzi*: implications for Chagas disease drug discovery and development, Sci. Rep. 4 (2014) 4703, https://doi.org/10.1038/srep04703.
[9] G. Yang, N. Lee, J.-R. Ioset, J.H. No, Evaluation of parameters impacting drug susceptibility in intracellular *Trypanosoma cruzi* assay protocols, SLAS Discovery 22 (2017) 125-134, https://doi.org/10.1177/1087057116673796.
[10] M. Cal, J.-R. Ioset, M.A. Fugi, P. Maser, M. Kaiser, Assessing anti-*T. cruzi* candidates *in vitro* for sterile cidality, Int. J. Parasitol. Drugs Drug Resist. 6 (2016) 165-170, https://doi.org/10.1016/j.ijpddr.2016.08.003.
[11] M. De Rycker, J. Thomas, J. Riley, S.J. Brough, T.J. Miles, D.W. Gray, Identification of trypanocidal activity for known clinical compounds using a new *Trypanosoma cruzi* hit-discovery screening cascade, PLoS Neglected Trop. Dis. 10 (2016) e0004584, https://doi.org/10.1371/journal.pntd.0004584.
[12] A.F. Francisco, M.D. Lewis, S. Jayawardhana, M.C. Taylor, E. Chatelain, J.M. Kelly, Limited ability of posaconazole to cure both acute and chronic *Trypanosoma cruzi* infections revealed by highly sensitive *in vivo* imaging. Antimicrob. Agents Chemother. 59 (2015) 4653-4661, https://doi.org/10.1128/AAC.00520-15.
[13] E.D. Deeks, Fexinidazole: first global approval, Drugs 79 (2019) 215-220, https://doi.org/10.1007/s40265-019-1051-6.
[14] A.F. Francisco, S. Jayawardhana, M.D. Lewis, K.L. White, D.M. Shackleford, G. Chen, J. Saunders, M. Osuna-Cabello, K.D. Read, S.A. Charman, E. Chatelain, J.M. Kelly, Nitroheterocyclic drugs cure experimental *Trypanosoma cruzi* infections more effectively in the chronic stage than in the acute stage, Sci. Rep. 6 (2016) 35351, https://doi.org/10.1038/srep35351.
[15] J.A. Watson, N. Strub-Wourgraft, A. Tarral, I. Ribeiro, J. Tarning, N.J. White, Pharmacokinetic-pharmacodynamic assessment of the hepatic and bone marrow toxicities of the new trypanoside fexinidazole, Antimicrob. Agents Chemother. 63 (2019) e02515-18, https://doi.org/10.1128/AAC.02515-18.
[16] Drugs for Neglected Diseases *initiative*, Fexinidazole for Chagas, Available at: https://dndi.org/research-development/portfolio/fexinidazole-for-chagas/ (accessed 30 August, 2020).
[17] R.T. Jacobs, J.J. Plattner, M. Keenan, Boron-based drugs as antiprotozoals, Curr. Opin. Infect. Dis. 24 (2011) 586-592, https://doi.org/10.1097/QCO.0b013e32834c630e

[18] M. Keenan, J.H. Chaplin, P.W. Alexander, M.J. Abbott, W.M. Best, A. Khong, A. Botero, C. Perez, S. Cornwall, R.A. Thompson, K.L. White, D.M. Shackleford, M. Koltun, F.C.K. Chiu, J. Morizzi, E. Ryan, M. Campbell, T.W. von Geldern, I. Scandale, E. Chatelain, S.A. Charman, Two analogues of fenarimol show curative activity in an experimental model of Chagas disease. J. Med. Chem. 56 (2013) 10158-10170, https://doi.org/10.1021/jm401610c.

[19] M.V. Papadopoulou, W.D. Bloomer, H.S. Rosenzweig, A.L. Mazzeti, K.R. Gonçalves, P.F. Mendes, M.T. Bahia, Nitrotriazole-based compounds as antichagasic agents in a long-treatment *in vivo* assay, Antimicrob. Agents Chemother. 61 (2017) e02717-16, https://doi.org/10.1128/AAC.02717-16.

[20] V. Ribeiro, N. Dias, T. Paiva, L. Hagström-Bex, N. Nitz, R. Pratesi, M. Hecht, Current trends in the pharmacological management of Chagas disease, Int. J. Parasitol. Drugs Drug Resist. 12 (2020) 7-17, https://doi.org/10.1016/j.ijpddr.2019.11.004.

[21] A.B. Vermelho, G.C. Rodrigues, C.T. Supuran, Why hasn't there been more progress in new Chagas disease drug discovery? Expert Opin. Drug Discov. 15 (2020) 145-158, https://doi.org/10.1080/17460441.2020.1681394.

[22] S. Khare, A.S. Nagle, A. Biggart, Y.H. Lai, F. Liang, L.C. Davis, S.W. Barnes, C.J.N. Mathison, E. Myburgh, M.Y. Gao, J.R. Gillespie, X. Liu, J.L. Tan, M. Stinson, I.C. Rivera, J. Ballard, V. Yeh, T. Groessl, G. Federe, H.X.Y. Koh, J.D. Venable, B. Bursulaya, M. Shapiro, P.K. Mishra, G. Spraggon, A. Brock, J.C. Mottram, F.S. Buckner, S.P.S. Rao, B.G. Wen, J.R. Walker, T. Tuntland, V. Molteni, R.J. Glynne, F. Supek, Proteasome inhibition for treatment of leishmaniasis, Chagas disease and sleeping sickness, Nature 537 (2016) 229-233, https://doi.org/10.1038/nature19339.

[23] P. Nagendar, J.R. Gillespie, Z.M. Herbst, R.M. Ranade, N.M.R. Molasky, O. Faghih, R.M. Turner, M.H. Gelb, F.S. Buckner, Triazolopyrimidines and imidazopyridines: structure-activity relationships and in vivo efficacy for trypanosomiasis, ACS Med. Chem. Lett. 10 (2019) 105-110, https://doi.org/10.1021/acsmedchemlett.8b00498.

[24] S.P.S. Rao, S.B. Lakshminarayana, J. Jiricek, M. Kaiser, R. Ritchie, E. Myburgh, F. Supek, T. Tuntland, A. Nagle, V. Molteni, P. Mäser, J.C. Mottram, M.P. Barrett, T.T. Diagana, Anti-trypanosomal proteasome inhibitors cure hemolymphatic and meningoencephalic murine infection models of African trypanosomiasis, Trop. Med. Infect. Dis. 5 (2020) 28; https://doi.org/10.3390/tropicalmed5010028.

[25] E. Chatelain, J.-R. Ioset, Phenotypic screening approaches for Chagas disease drug discovery, Expert Opin. Drug Discov. 13 (2018) 141-153, https://doi.org/10.1080/17460441.2018.1417380.

[26] D.M. Klug, M.H. Gelb, M.P. Pollastri, Repuposing strategies for tropical disease drug discovery, Bioorg. Med. Chem. Lett. 26 (2016) 2569-2576, https://doi.org/10.1016/j.bmcl.2016.03.103.

[27] S.J. Keam, Pretomanid: first approval, Drugs 79 (2019) 1797-1803, https://doi.org/10.1007/s40265-019-01207-9.

[28] Drugs for Neglected Diseases *initiative*, Drug discovery, Available at: https://dndi.org/research-development/drug-discovery/ (accessed 7 September, 2020).

[29] TB Alliance discovery, Available at: https://www.tballiance.org/rd/discovery (accessed 7 September, 2020).

[30] A.M. Thompson, P.D. O'Connor, A. Blaser, V. Yardley, L. Maes, S. Gupta, D. Launay, D. Martin, S.G. Franzblau, B. Wan, Y. Wang, Z. Ma, W.A. Denny, Repositioning antitubercular 6-nitro-2,3-dihydroimidazo[2,1-*b*][1,3]oxazoles for neglected tropical diseases: structure–activity studies on a preclinical candidate for

visceral leishmaniasis, J. Med. Chem. 59 (2016) 2530-2550, https://doi.org/10.1021/acs.jmedchem.5b01699.
[31] A.M. Thompson, P.D. O'Connor, A.J. Marshall, V. Yardley, L. Maes, S. Gupta, D. Launay, S. Braillard, E. Chatelain, S.G. Franzblau, B. Wan, Y. Wang, Z. Ma, C.B. Cooper, W.A. Denny, 7-Substituted 2-nitro-5,6-dihydroimidazo[2,1-*b*][1,3]oxazines: novel antitubercular agents lead to a new preclinical candidate for visceral leishmaniasis, J. Med. Chem. 60 (2017) 4212-4233, https://doi.org/10.1021/acs.jmedchem.7b00034.
[32] M. Keenan, M.J. Abbott, P.W. Alexander, T. Armstrong, W.M. Best, B. Berven, A. Botero, J.H. Chaplin, S.A. Charman, E. Chatelain, T.W. von Geldern, M. Kerfoot, A. Khong, T. Nguyen, J.D. McManus, J. Morizzi, E. Ryan, I. Scandale, R.A. Thompson, S.Z. Wang, K.L. White, Analogues of fenarimol are potent inhibitors of *Trypanosoma cruzi* and are efficacious in a murine model of Chagas disease, J. Med. Chem. 55 (2012) 4189-4204, https://doi.org/10.1021/jm2015809.
[33] B.D. Palmer, A.M. Thompson, H.S. Sutherland, A. Blaser, I. Kmentova, S.G. Franzblau, B. Wan, Y. Wang, Z. Ma, W.A. Denny, Synthesis and structure-activity studies of biphenyl analogues of the tuberculosis drug (6*S*)-2-nitro-6-{[4-(trifluoromethoxy)benzyl]oxy}-6,7-dihydro-5*H*-imidazo[2,1-*b*][1,3]oxazine (PA-824), J. Med. Chem. 53 (2010) 282-294, https://doi.org/10.1021/jm901207n.
[34] A.M. Thompson, A. Blaser, R.F. Anderson, S.S. Shinde, S.G. Franzblau, Z. Ma, W.A. Denny, B.D. Palmer, Synthesis, reduction potentials, and antitubercular activity of ring A/B analogues of the bioreductive drug (6*S*)-2-nitro-6-{[4-(trifluoromethoxy)benzyl]oxy}-6,7-dihydro-5*H*-imidazo[2,1-*b*][1,3]oxazine (PA-824), J. Med. Chem. 52 (2009) 637-645, https://doi.org/10.1021/jm801087e.
[35] A.M. Thompson, A. Blaser, B.D. Palmer, R.F. Anderson, S.S. Shinde, D. Launay, E. Chatelain, L. Maes, S.G. Franzblau, B. Wan, Y. Wang, Z. Ma, W.A. Denny, 6-Nitro-2,3-dihydroimidazo[2,1-*b*][1,3]thiazoles: facile synthesis and comparative appraisal against tuberculosis and neglected tropical diseases, Bioorg. Med. Chem. Lett. 27 (2017) 2583-2589, https://doi.org/10.1016/j.bmcl.2017.03.069.
[36] A.M. Thompson, H.S. Sutherland, B.D. Palmer, I. Kmentova, A. Blaser, S.G. Franzblau, B. Wan, Y. Wang, Z. Ma, W.A. Denny, Synthesis and structure-activity relationships of varied ether linker analogues of the antitubercular drug (6*S*)-2-nitro-6-{[4-(trifluoromethoxy)benzyl]oxy}-6,7-dihydro-5*H*-imidazo[2,1-*b*][1,3]oxazine (PA-824), J. Med. Chem. 54 (2011) 6563-6585, https://doi.org/10.1021/jm200377r.
[37] A.M. Thompson, A.J. Marshall, L. Maes, N. Yarlett, C.J. Bacchi, E. Gaukel, S.A. Wring, D. Launay, S. Braillard, E. Chatelain, C.E. Mowbray, W.A. Denny, Assessment of a pretomanid analogue library for African trypanosomiasis: hit-to-lead studies on 6-substituted 2-nitro-6,7-dihydro-5*H*-imidazo[2,1-*b*][1,3]thiazine 8-oxides, Bioorg. Med. Chem. Lett. 28 (2018) 207-213, https://doi.org/10.1016/j.bmcl.2017.10.067.
[38] A.M. Thompson, A. Blaser, B.D. Palmer, S.G. Franzblau, B. Wan, Y. Wang, Z. Ma, W.A. Denny, Biarylmethoxy 2-nitroimidazooxazine antituberculosis agents: effects of proximal ring substitution and linker reversal on metabolism and efficacy, Bioorg. Med. Chem. Lett. 25 (2015) 3804-3809, https://doi.org/10.1016/j.bmcl.2015.07.084.
[39] W.R. Baker, C. Shaopei, E.L. Keeler, Nitro-[2,1-b]imidazopyran compounds and antibacterial uses thereof, U.S. Patent 6087358 (2000), Available at: https://patents.google.com/patent/US6087358A/en.
[40] I. Kmentova, H.S. Sutherland, B.D. Palmer, A. Blaser, S.G. Franzblau, B. Wan, Y. Wang, Z. Ma, W.A. Denny, A.M. Thompson, Synthesis and structure-activity relationships of aza- and diazabiphenyl analogues of the antitubercular drug (6*S*)-2-

nitro-6-{[4-(trifluoromethoxy)benzyl]oxy}-6,7-dihydro-5*H*-imidazo[2,1-*b*][1,3]oxazine (PA-824), J. Med. Chem. 53 (2010) 8421-8439, https://doi.org/10.1021/jm101288t.

[41] O. Longin, H. van de Langemheen, R.M.J. Liskamp, An orthogonally protected CycloTriVeratrylene (CTV) as a highly pre-organized molecular scaffold for subsequent ligation of different cyclic peptides towards protein mimics, Bioorg. Med. Chem. 25 (2017) 5008-5015, https://doi.org/10.1016/j.bmc.2017.05.038.

[42] N. Iranpoor, H. Firouzabadi, A.A. Jafari, A green protocol for the easy synthesis of thiiranes from epoxides using thiourea/silica gel in the absence of solvent, Phosphorus Sulfur Silicon Relat. Elem. 180 (2005) 1809-1814, https://doi.org/10.1080/104265090889404.

[43] M. Muehlbacher, C.D. Poulter, Regioselective opening of simple epoxides with diisopropylamine trihydrofluoride, J. Org. Chem. 53 (1988) 1026-1030, https://doi.org/10.1021/jo00240a017.

[44] S. Patterson, S. Wyllie, L. Stojanovski, M.R. Perry, F.R.C. Simeons, S. Norval, M. Osuna-Cabello, M. De Rycker, K.D. Read, A.H. Fairlamb, The *R* enantiomer of the antitubercular drug PA-824 as a potential oral treatment for visceral leishmaniasis, Antimicrob. Agents Chemother. 57 (2013) 4699-4706, https://doi.org/10.1128/AAC.00722-13.

[45] A.M. Thompson, P.D. O'Connor, A.J. Marshall, A. Blaser, V. Yardley, L. Maes, S. Gupta, D. Launay, S. Braillard, E. Chatelain, B. Wan, S.G. Franzblau, Z. Ma, C.B. Cooper, W.A. Denny, Development of (6*R*)-2-nitro-6-[4-(trifluoromethoxy)phenoxy]-6,7-dihydro-5*H*-imidazo[2,1-*b*][1,3]oxazine (DNDI-8219): a new lead for visceral leishmaniasis, J. Med. Chem. 61 (2018) 2329-2352, https://doi.org/10.1021/acs.jmedchem.7b01581.

[46] J. Riley, S. Brand, M. Voice, I. Caballero, D. Calvo, K.D. Read, Development of a fluorescence-based *Trypanosoma cruzi* CYP51 inhibition assay for effective compound triaging in drug discovery programmes for Chagas disease, PLoS Neglected Trop. Dis. 9 (2015) e0004014, https://doi.org/10.1371/journal.pntd.0004014.

[47] M.L. Sykes, V.M. Avery, Development and application of a sensitive, phenotypic, high-throughput image-based assay to identify compound activity against *Trypanosoma cruzi* amastigotes, Int. J. Parasitol. Drugs Drug Resist. 5 (2015) 215-228, https://doi.org/10.1016/j.ijpddr.2015.10.001.

[48] S. Patterson, A.H. Fairlamb, Current and future prospects of nitro-compounds as drugs for trypanosomiasis and leishmaniasis, Curr. Med. Chem. 26 (2019) 4454-4475, https://doi.org/10.2174/0929867325666180426164352.

[49] S. Wyllie, A.J. Roberts, S. Norval, S. Patterson, B.J. Foth, M. Berriman, K.D. Read, A.H. Fairlamb, Activation of bicyclic nitro-drugs by a novel nitroreductase (NTR2) in *Leishmania*, PLoS Pathog. 12 (2016) e1005971, https://doi.org/10.1371/journal.ppat.1005971.

[50] A.Y. Sokolova, S. Wyllie, S. Patterson, S.L. Oza, K.D. Read, A.H. Fairlamb, Cross-resistance to nitro drugs and implications for treatment of human African trypanosomiasis, Antimicrob. Agents Chemother. 54 (2010) 2893-2900, https://doi.org/10.1128/AAC.00332-10.

[51] B.S. Hall, S.R. Wilkinson, Activation of benznidazole by trypanosomal type I nitroreductases results in glyoxal formation, Antimicrob. Agents Chemother. 56 (2012) 115-123, https://doi.org/10.1128/AAC.05135-11.

[52] M.D. Lewis, A.F. Francisco, M.C. Taylor, J.M. Kelly, A new experimental model for assessing drug efficacy against *Trypanosoma cruzi* infection based on highly sensitive

in vivo imaging, J. Biomol. Screening 20 (2015) 36-43, https://doi.org/10.1177/1087057114552623.
[53] A.W. Basit, J.M. Newton, M.D. Short, W.A. Waddington, P.J. Ell, L.F. Lacey, The effect of polyethylene glycol 400 on gastrointestinal transit: implications for the formulation of poorly-water soluble drugs, Pharm. Res. 18 (2001) 1146-1150, https://doi.org/10.1023/a:1010927026837.